Pan-Arctic soil element bioavailability estimations

Peter Stimmler[1], Mathias Goeckede[2], Bo Elberling[3], Susan Natali[4], Peter Kuhry[5], Nia Perron[6], Fabrice Lacroix[2], Gustaf Hugelius[5,7], Oliver Sonnentag[6], Jens Strauss[8], Christina Minions[4], Michael Sommer[1], and Jörg Schaller[1*]

[1] Leibniz Centre for Agricultural Landscape Research (ZALF), Müncheberg, Germany
[2] Max Planck Institute for Biogeochemistry, Jena, Germany
[3] Center for Permafrost, Department of Geosciences and Natural Resource Management, University of Copenhagen, Copenhagen, Denmark
[4] Woodwell Climate Research Center, Falmouth, USA
[5] University Stockholm, Stockholm, Sweden
[6] Département de Géographie, Université de Montréal, 1375 Avenue Thérèse-Lavoie-Roux, Montréal, QC H2V 0B3, Canada
[7] Bolin Centre for Climate Research, Stockholm University, Stockholm, Sweden
[8] Alfred Wegener Institute Helmholtz Centre for Polar and Marine Research, Permafrost Research Section, Potsdam, Germany

** Correspondence to: email: Joerg.Schaller@zalf.de*

Abstract. Arctic soils store large amounts of organic carbon and other elements such as amorphous silicon, silicon, calcium, iron, aluminium, and phosphorous. Global warming is projected to be most pronounced in the Arctic leading to thawing permafrost, which in turn is changing the soil element availability. To project how biogeochemical cycling in Arctic ecosystems will be affected by climate change, there is a need for data on element availability. Here, we analysed the amorphous silicon (ASi) content as solid fraction of the soils, as well as Mehlich III extractions for bioavailability of silicon (Si), calcium (Ca), iron (Fe), phosphorus (P), and aluminium (Al) from 574 soil samples from the circumpolar Arctic region. We show large differences in ASi fraction and Si, Ca, Fe, Al, and P availability among different lithologies and Arctic regions. We summarized these data in pan-Arctic maps of ASi fraction and available Si, Ca, Fe, P, and Al concentrations focussing on the top 100 cm of Arctic soil. Furthermore, we provide values for element availability for the organic and the mineral layer of the seasonally thawing active layer as well as for the uppermost permafrost layer. Our spatially explicit data on differences in the availability of elements between the different lithological classes and regions now and in the future will improve Arctic Earth system models for estimating current and future carbon and nutrient feedbacks under climate change.

Gelöscht: silica

Gelöscht: silica

Gelöscht: silicon minerals

Gelöscht: as silicic acid

Gelöscht: availability

Gelöscht:

Gelöscht: ,

Gelöscht: P,

Gelöscht: Al

Gelöscht: ,

1 Introduction

Temperatures in northern high latitude region have risen more than twice as fast as the global average within the last decades (IPCC, 2021). This warming leads to thawing of perennially frozen ground known as permafrost (Brown and Romanovsky, 2008; Romanovsky et al., 2010). Frozen conditions prevent organic matter (OM) from microbial degradation and also limits fluvial export of soil-bound nutrients to the sea by runoff (Mann et al., 2022). Thawing of permafrost soils may in turn accelerate global warming by potentially releasing potent greenhouse gases such as carbon dioxide (CO_2) and methane (CH_4) through soil organic carbon mineralization (Schuur et al., 2015). The frozen ground of the Arctic-boreal regions (hereafter called 'Arctic', but also including subarctic regions) are the largest pool of soil organic carbon worldwide. Approximately, 1014 - 1035 ± max. 194 Pg of organic carbon is stored within the upper 3 m of permafrost region soils (Hugelius et al., 2014; Mishra et al., 2021) (Hugelius et al., 2014; Mishra et al., 2021). To full depth, ca. 1460 - 1600 Pg of organic carbon is stored in the permafrost region (Strauss, 2021), and approximately one third of this is in ice rich Yedoma deposits, exceeding 3 m depth (Fuchs et al., 2018; Strauss et al., 2017b). The Yedoma deposits formed in unglaciated areas of the northern hemisphere during the glacial period, when melt water from glacial areas and eolian processes transported fine sediment to the unglaciated lowlands (Schuur et al., 2013; Strauss, 2021; Strauss et al., 2013). Yedoma deposits are characterized by high carbon and water content. The water is mostly bound in massive ice in ice wedges as well as segregated ice and pore ice in sediment columns (Schirrmeister et al., 2011). Thus, Yedoma soils are highly vulnerable to thawing as the loss of the high ice volume leads to surface subsidence and thermokarst processes, which can accelerate thaw and remobilize deep elemental stocks.

Low temperatures in the Arctic systems slow down biological and chemical processes and preserve OM for millennia (Sher et al., 2005). Due to Arctic warming these processes are accelerated by an increased nutrient and OM mobilization from the permafrost (Salmon et al., 2016). Consequently, OM may become vulnerable to respiration (Hugelius et al., 2020; Strauss et al., 2017b). The temperature and near-surface water content in the Arctic soils have changed rapidly in the last decades and further changes are expected in future (Box et al., 2019). An important effect of Arctic warming is a deepening of the seasonally-thawed active layer and related thermokarst processes, which may lead to a mobilization of nutrients from permafrost soil layers (Abbott et al., 2015). Additionally, increased temperatures in the Arctic regions may accelerate weathering, potentially enhancing nutrient availability in terrestrial Arctic ecosystems and export to freshwater systems, and finally to the nearshore zone and sea (Goldman et al., 2013). As the Arctic features a mineral composition of the soils that is different from many other global soils (Monhonval et al., 2021), the availability (for microbes and plants) of elements in Arctic soils may differ as well. Yedoma deposits, for example, are important pools of OM in the Arctic. Because Yedoma deposits include materials transported from nearby mountains, the mineral compositions of these Yedoma deposits depend on the original geology of the mountains (Schirrmeister et al., 2011). Further, sediments of marine origin are often rich in available calcium (Ca), phosphorus (P) and silicic acid (Si), while magmatic rocks such as granite or basalt contain large amounts of Si, iron (Fe), aluminum (Al), and P. The complex mineral composition of fluvial and marine sediments is reflected in the element availability of the soils formed from these deposits. The availability of these elements in soils is the complex product of soil genesis, nutrient release and plant cycling. The soil properties and the vegetation type interact in terms

Gelöscht: frozen ground (defined as
Gelöscht: in the following)
Gelöscht:
Gelöscht:
Gelöscht: ±
Gelöscht:
Gelöscht:
Gelöscht:
Gelöscht: ¶
Gelöscht: sediments
Gelöscht: he Yedoma soils
Gelöscht: S
Gelöscht: silicon
Gelöscht: and
Gelöscht: ,
Gelöscht: and external inputs,

of *Sphagno-Eriophorum vaginati* potentially lead to Si accumulation in the uppermost soil layer of the moist acidic tundra, whereas in the moist non-acidic tundra the *Dryado integrifoliae-Caricetum* may lead to an accumulation of Ca in the uppermost soil layer (Walker et al., 2001). Further, external inputs, e.g. by fluvial transport in Yedoma regions, may alter soil genesis and element availability (Monhonval et al., 2021; Strauss et al., 2017a). These processes depend on physical and chemical conditions including temperature, water content and pH. In this context, Si, Ca, Fe, Al or P are bound in or on mineral phases and are released via enzymatic activity or weathering. Ongoing Arctic climate warming now threatens to disturb the pools that have equilibrated to conditions characteristic for the past millennia.

Nutrient availability (easily available share of elements for potential uptake in plants within short time span e.g. days, not month) is important to meet the plants requirements in terms of nutrition as only optimal nutrition will result in high biomass production. The availability of elements such as P, Fe, Ca, and Si in soils are known controls for soil OM respiration (Weil and Brady, 2017). A release of inorganic nutrients such as P or Si can lead to increased greenhouse gas production and potentially to further export of these elements to the fresh and seawaters. In marine systems, P, Fe, Ca, and Si are well-known to control carbon (C) fixation in terms of algae biomass productivity (Tremblay et al., 2015). In terrestrial systems, P availability is positively related to Si (Schaller et al., 2019) or its polymers, which mobilize from, e.g., ASi (Stimmler et al., 2021). The mobilization of P by Si was shown to occur due to competition for binding at Fe-minerals (Schaller et al., 2019), which tend to strongly bind P under condition of low Si availability (Gérard, 2016). Contrary to Si, Ca binds P by calcium phosphate co-precipitation with calcium carbonate, at least under high soil pH conditions (Otsuki and Wetzel, 1972). Like P, OM is also binding to Ca, Fe and Al-phases (Kaiser and Zech, 1997; Wiseman and Püttmann, 2006) but being mobilized from those phases by Si (Hömberg et al., 2020). If the Fe availability in soils is low, the binding of P may be related to Al-minerals (Eriksson et al., 2015).

Despite the important role of soil elements in driving soil and ecosystem processes and the potential for rapid changes in the Arctic due to climate change, the spatial distribution of elemental stocks (beyond C, N) is not well understood. An ecologically based classification of soil Ca concentrations was proposed by (Walker et al., 2001), differentiating between a Ca rich non-acidic tundra and a Ca poor acidic tundra based on differences in vegetation types for the Alaskan Arctic region. This classification system was further used to estimate pan-Arctic soil OM stocks (Hugelius et al., 2014), which proved to be a useful approach as vegetation is tightly connected to OM stocks (Quideau et al., 2001). Based on the work of (Hugelius et al., 2014), (Alfredsson et al., 2016) related vegetation cover to ASi concentration to scale up Arctic ASi stocks. However, in contrast to OM stocks being clearly related to vegetation (Hugelius et al., 2014), the vegetation might have an effect on mineral availability in soils (Villani et al., 2022). It is known that soils dominated by sedges may become enriched in available Si, whereas soils dominated by shrub vegetation may become enriched in available Ca (Mauclet et al., 2022). Climate change driven alterations in vegetation communities may lead to changed element availabilities in Arctic soils. Other elements like P and Ca are cycled by plant intensively and by this becoming enriched in the uppermost soil layer (Jobbágy and Jackson, 2001). This points to the importance of biogeochemical interactions between vegetation and soil. However, this approach does not account for the inorganic element pool, dominated by the bedrock geology initially. Therefore, the extrapolation of circum-polar Arctic maps

Gelöscht: ,
Gelöscht: in moist acidic tundra
Gelöscht: es Si
Gelöscht: es high concentrations of available
Gelöscht: can
Gelöscht: modify
Gelöscht:
Gelöscht: ,
Gelöscht: which depend
Gelöscht: i
Gelöscht: silicic acid ($Si(OH)_4$)
Gelöscht: amorphous silica (
Gelöscht: amorphous Si (
Gelöscht:)
Gelöscht: effect of
Gelöscht: is
Gelöscht: is
Gelöscht: changes
Gelöscht: by this will
Gelöscht: more
Gelöscht: getting
Gelöscht: first 20 cm of the
Gelöscht: out
Gelöscht: , but if vegetation has a dominant effect and how long it takes to change mineral availability in soils by vegetation is debatable
Gelöscht: into

of element availability for P, Fe, Ca, Al, and Si based on vegetation distribution alone may be associated with high uncertainties. A much stronger driver of element availability could be parent material and lithology (Alloway, 2013). In this study, we aim to map pan-Arctic soil element bio-availability (for microbes and plants) by applying a lithology-based extrapolation of plot level sampling data on nutrient availability. We provide maps for the solid ASi fraction and available Si, Ca, Fe, P and Al concentrations as these elements have direct effects on OM binding and greenhouse gas (GHG) emission from the circumpolar Arctic. In addition, these elements, once transported to the marine systems, may affect primary production by diatoms and coccolithophores, as some of those nutrients are limiting for those algae and hence limiting CO_2 binding due to algae biomass production. Better understanding of element availability is crucial to reduce uncertainties for reliable modelling of future scenarios on how Arctic system may respond to global warming.

Gelöscht: ,

Gelöscht: are limiting nutrients for CO2 binding in terms of

Gelöscht: In addition, these elements are limiting nutrients for CO2 binding in terms of primary production in Arctic marine systems by Fe and P being main nutrients and both Si and Ca are important for biomass production of either diatoms or coccolithophores or interfere with those.

2 Material and Methods

2.1 General approach

Based on the Geological Map of the Arctic (Harrison et al., 2011), we estimate the bio-availability and potential mobility of Si, Ca, Fe, Al and P as well as solid ASi fraction in Arctic soils. We analyzed soil samples from organic, mineral and permafrost layers from pan-Arctic sampling campaigns. We used the biological available element concentrations for mineral Si, Ca, Fe, Al, P and solid ASi fraction of certain lithologies to compile pan-Arctic maps covering 7.6x106 km².

2.2 Sampling and storage

In total, we analyzed 574 Arctic soil samples from 25 locations taken over a period of one decade (Fig. 1). To ensure a pan-Arctic coverage we analyzed samples from Siberia (222 samples from six locations), North America (115 samples from six locations), Greenland (111 samples from nine locations), Northern Europe (13 samples from one location) and Svalbard (103 samples from three locations) (Fig. 1 and S1, Table S1). We analyzed samples from the thawed near-surface organic layer (252 soil samples, mainly 0-20 cm in depth), mineral layer (208 soil samples, mainly 20 – 50 cm depth)) and permafrost layer (104 soil samples, mainly 50 – 100 cm depth). The sampling designs accounted for the spatial variation of single locations (several samples were taken on ~1 km transects. Repeated sampling of month to decades was not possible. We split the annually thawed active layer in the upper organic layer and the mineral layer below by C content, except for soils where the organic layer corresponds to the active layer. The organic layer contained mainly organic matter (OM) in different mineralization states. The mineral soil layer has variable OM content depending on which soil processes have affected this layer and reaches to the perennially frozen permafrost layer. We took samples using an auger or a spade and stored them frozen until analysis or as described before (Faucherre et al., 2018; Kuhry et al., 2020). Samples consisted of 5-50 g frozen soil. Before analysis, the samples were freeze dried for 48 hours and ground. The freeze drying inhibits thermal degradation of the soil material and is standard for the Mehlich III extraction and alkaline extraction described below.

2.3 Extraction and analysis

Mehlich III extractions for available element concentrations.

Available concentrations of Si, Ca, Fe, Al and P were quantified using the Mehlich III method (Sims, 1989). The Mehlich III is extracting the silicic acid which is adsorbed to the soil particle surface and the free silicic acid. For the elements Ca, Fe, Al and P the extract is defined as *biological available share of the analysed elements*, in the script labelled as "*available*". This fraction includes the element concentrations solved in the pore water and the fraction adsorbed to organic and inorganic soil particles. Microbes and plants care able to mobilize this adsorbed share of nutrients. We defined the extraction method Mehlich III to reflect this available element concentrations. Briefly, we extracted 0.5 to 5 g of freeze-dried soil using 10 ml g-1 Mehlich III solution (0.015 M NH_4F, 0.001 M EDTA, 0.25 M

Gelöscht: ASi,

Gelöscht: for ASi, mineral Si, Ca, Fe, Al and P.

Gelöscht: ¶

Gelöscht:

Gelöscht:

Gelöscht:

Gelöscht:

Gelöscht:

Gelöscht:

Gelöscht:

Gelöscht:

Gelöscht: -

Gelöscht:

Gelöscht:

Gelöscht: -

Gelöscht:

Gelöscht: took

Gelöscht: into account

Gelöscht: ,

Gelöscht: a temporal r

Gelöscht: was not done

Gelöscht:

Gelöscht: oven

Gelöscht: at 40°C

Gelöscht: etraction the

Gelöscht: *mineral*

Gelöscht: the concentrations in

Gelöscht: are

Gelöscht: named

Gelöscht: an

Gelöscht: and by this increase the pool of nutrients

NH_4NO_3, 0.00325 M HNO_3, 0.2 M HAc). The samples were shaken for 5 min at 200 min-1 and centrifuged for 5 min at 10.000 x g. Afterwards the supernatant was filtered using a 0.2 µm cellulose acetate filter. The concentration of Si, Ca, Fe, Al and P was measured by inductive coupled plasma with optical emission spectroscopy (ICP-OES) (Vista-PRO radial, Varian Medical Systems, Palo Alto, California).

Alkaline extraction for solid fraction of amorphous silicon.

For extraction of solid amorphous silicon (ASi) fraction an alkaline extraction was used (DeMaster, 1981), extracting ASi from 30 mg of freeze-dried soil using 40 ml 0.1 M Na_2CO_3 solution at 85°C for 5 h. After 1 h, 3 h and 5 h the suspension was mixed, and 10 ml of the supernatant was subsampled, filtered by a 0.2 µm cellulose acetate filter and analyzed by ICP-OES (Vista-PRO radial, Varian Medical Systems, Palo Alto, California). The ASi concentration was calculated using a linear regression of ASi concentration in solution over time and the intersection with the Y-axis was used as concentration of available concentration according to (DeMaster, 1981). The Mehlich III extract was used to determine the available concentrations of the elements and the alkaline extraction was used to determine the pool of particulate amorphous silicon in the soil. To determine the dry weight (DW) of the samples 0.5-2 g of frozen material was freeze dried until weight constancy.

2.4 Statistics

2.4.1 Statistics and graphics

Data were analyzed using the R Studio (R Core Team, 2022). We extracted the original data (lithology, location, geometry) given for GIS polygons (shape files from the different regions, Greenland, Can_USA, Ice, N_Europa_Russia) of the Geological Map of the Arctic containing locations. We extracted 14 lithological classes in total. We matched the soil sampling locations for which we obtained data for element availability by extraction (see above) with the GIS polygons (geology) by ARCView_GIS_3.2 extensions "Spatial Analyst" command "analysis: tabulate Areas". The sum of areas with the same map label was extracted by map label "shape area". We considered only terrestrial areas. For every location, we calculated the mean available element concentrations for ASi, Si, Ca, Fe, Al and P with bootstrapping (boot=1000) for the organic, mineral and permafrost layer. We calculated quantiles, mean and standard error using "summarise" from the "dplyr" R package. We clustered available element concentration data for all locations by lithological class and calculated mean and standard error for organic, mineral and permafrost layer. The number of samples for each lithological class is given in Fig. 1.

2.4.2 Element concentration maps

We used the "Geological Map of the Arctic (1:5 000 000 scale, in the Arctic polar region, north of latitude 60°N") as the basis for our maps. We calculated the weighted numeric mean concentration for each element in the first 100 cm from the soil surface using equation (1). The mean mass fraction (wm) of an element (X) is the sum of the products of the mass fractions in organic (OL), mineral (ML) and permafrost (PL) layer and the thickness (d) of each layer in cm divided by 100 cm. We colored the represented area based on the element concentration.

$$w_m\,(X)\,\left[\frac{mg}{g}\right] = \frac{(w_{OL}(X)\left[\frac{mg}{g}\right]*d_{OL}\,[m] + w_{ML}(X)\left[\frac{mg}{g}\right]*d_{ML}\,[m] + w_{PL}(X)\left[\frac{mg}{g}\right]*d_{PL}\,[cm])}{100\,[cm]} \qquad \text{(eq. 1)}$$

Gelöscht:
Gelöscht:
Gelöscht:
Gelöscht: ,
Gelöscht: The analysis was done by
Gelöscht: available
Gelöscht: silica
Gelöscht: (DeMaster 1981)
Gelöscht:
Gelöscht: DeMaster (1981)
Gelöscht: silica
Gelöscht:
Gelöscht: ¶
Gelöscht: the different samples f
Gelöscht: from
Gelöscht: ¶
Gelöscht:
Gelöscht:
Gelöscht: formula

3 Results

3.1 Geographical and lithological representation

Our sampling locations represent 13 out of 17 original geographic domains (missing: North Asia and North America, ice, none assigned), defined by the base map (76.5 %) (Table 1, Fig. S1 and Table S2) of the Arctic. The single areas and shares for the maps of Canada/Alaska, Greenland and North Europe/Russia are given in Table S3. Our data represent 17 periods of the Geological Map of the Arctic. The age ranged between 2.6 and 2,500 mya. The number of samples per age code are shown in Fig S2. Our data represent 14 lithological classes of the "Geological Map of the Arctic" (Table S4). These 14 lithological classes represent 7.63×10^{12} m² out of 1.57×10^{13} m² (48.49 % of the area represented by the Geological Map of the Arctic, including ice sheets). Sediments cover 1.03×10^{13} m² of the Arctic. Our data represent sedimentary classes that cover 6.77×10^{12} m² (65.9 % of the Arctic sediment cover) (Fig. S3). In total 3.68×10^{11} m² of 7.37×10^{11} m² (49.9 %) of Yedoma deposits were represented (Fig. S4). The 14 lithological classes can be observed in the igneous type (extrusive: mafic. class 1, n=26), type unclassified (Metamorphic undivided: class 2, n=21) and the sedimentary type (Carbonate: class 3, n=24; class 4, n=58; class 5, n=64; Clastic: shallow marine: class 6, n=13; Clastic: deltaic and nearshore: class 7, n=68; Sedimentary: undivided: class 8, n=38; class 9, n=39; Clastic: shallow marine: class 10, n=91; class 11, n=60; Sedimentary and/or volcanic: undivided: class 12, n=21; and Slope and deep water: class 13, n=43; class 14, n=8).

Gelöscht: epochs

Gelöscht: eras

Gelöscht:

Table 1: Coverage of the areas of geographical domain, epochs, represented area, lithological class, sediments and Yedoma deposition by our data. First column lists original parameters given by the Geological Map of the Arctic (Harrison et al., 2011) and Yedoma deposits (Strauss et al., 2021). The column "Represented" gives absolute numbers for chronological or lithological classes extrapolated by this study. The represented area is the share of the entire area of the Arctic according to the Geological map used in this study for the listed parameters.

Parameter	Represented	Explanation	Example
Geographic domain	13 (76.5%)	"Phanerozoic regions are based on major physiographic features of the Arctic" (Harrison et al., 2011)	Interior western Alaska
Epochs	17 (2.6 – 2,500 mya)	"Standardization of map-unit attributes has been facilitated by the International Stratigraphic Chart (August 2009 version) published by the International Commission on Stratigraphy (ICS)" (Harrison et al., 2011)	Neogene (23.0 - 2.6 Ma)
Represented area	7.63×10^{12} m² (43.03%)	Area of the Geological Map of the Arctic (Harrison et al., 2011) containing own data to element concentrations (Fig. 3-8).	
Lithological class	14	Specification and examples of rock type	Lithological class 2: Gneiss, migmatite; reworked amphibolite and granulite facies rocks
Sediments	6.77×10^{12} m² (65.9%)	Areas with lithological classes of the sedimentary type	Lithological class 7: Sandstone, siltstone, shale, coal; plant fossils; metamorphic grade not identified
Yedoma deposition	3.68×10^{11} m² (49.9%)	Areas that contain Yedoma deposits defined by Strauss et al. (2021b)	

Gelöscht: and of the area

Gelöscht: from

Gelöscht: of the Arctic presented

Gelöscht: "

Gelöscht: For the area, relative share in comparison to total area given by original studies is given, too

Gelöscht: .

Gelöscht: Era

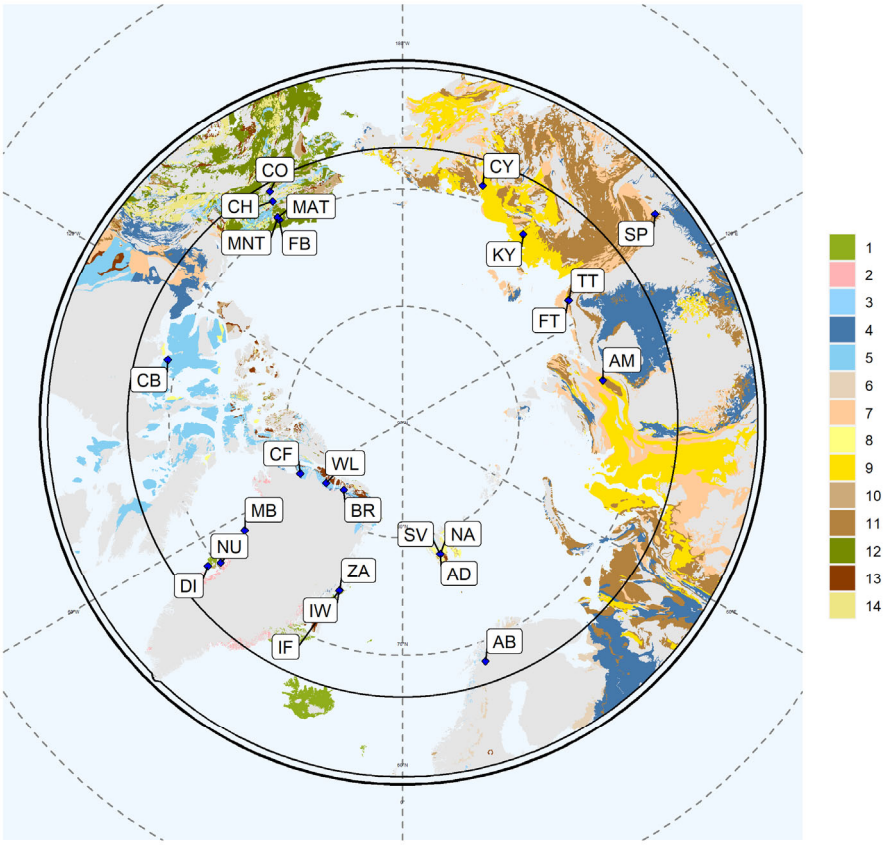

Fig. 1: Map of represented lithologies. The Arctic Circle (66.6°N) is included as a black circle. Each color represents a bedrock lithology: 1: Basalt, olivine basalt, tholeiite, alkali basalt, basanite, pillow basalt, flood basalt (n=26); 2: Gneiss, migmatite; reworked amphibolite and granulite facies rocks (n=11); 3: Limestone, dolostone, shale, evaporites, chalk; carbonate reefs or metamorphosed equivalent (n=24); 4: Limestone, dolostone, shale, evaporites, chalk; carbonate reefs; metamorphic grade not identified (n=58); 5: Limestone, dolostone, shale, evaporites, chalk; carbonate reefs (n=64); 6: Quartz sandstone, siltstone, claystone, limestone, dolostone, conglomerate, tillite (n=13); 7: Sandstone, siltstone, shale, coal; plant fossils; metamorphic grade not identified (n=68); 8: Sandstone, siltstone, shale, limestone (n=38); 9: Sandstone, siltstone, shale, limestone; metamorphic grade not identified (n=39); 10:

Gelöscht: extrapolated element concentrations

Sandstone, siltstone, shale; marine fossils (n=91); 11: Sandstone, siltstone, shale; marine fossils; metamorphic grade not identified (n=60); 12: Sedimentary and/or volcanic rock: undivided (n=21); 13: Shale, chert, iron-formation, greywacke, turbidite, argillaceous limestone, matrix-supported conglomerate (n=43); 14: Shale, chert, iron-formation, greywacke, turbidite, argillaceous limestone, matrix-supported conglomerate or metamorphosed equivalent (n=8). Grey color means areas of base map that are not represented by our data on element concentrations. Abbreviations for locations: CH: Alaska, Chandalar; CO: Alaska, Coldfoot; FB: Alaska, Franklin Bluff-Dry; MAT: Alaska, Moist acidic tundra; MNT: Alaska, Moist non-acidic tundra; CB: Canada, Cambridge Bay; BR: Greenland, Brønlund; CF: Greenland, Cass Fjord; DI: Greenland, Disko; MB: Greenland, Melville Bay; NU: Greenland, Nussuaq; WL: Greenland, Warming Land; ZA: Greenland, Zackenberg; IW: Greenland, Zackenberg, Ice Wedge; IF: Greenland, Zackenberg, Infilling Fan; AM: Russia, Ary-Mas; CY: Russia, Chersky; KY: Russia, Kytalyk; FT: Russia, Lena delta, first terrace; TT: Russia, Lena Delta, third terrace; SP: Russia, Spasskaya; AB: Sweden, Abisko; AD: Svalbard, Adventalen; NA: Svalbard, Adventalen; SV: Svalbard. This map is based on the Geological Map of the Arctic (Harrison et al., 2011).

3.2 Element availabilities across lithological classes at 0-1 m depth

The lithological classes differed substantially in their element availabilities (Fig. 2; Fig S5):

- We found a large range in **ASi concentrations** in the Arctic covering values from 0.03±0 mg g^{-1} DW ASi to 6.68±1.17 mg g^{-1} DW ASi. The highest concentrations of ASi were found in basalt and associated rock (class 1: 6.68±1.17 mg g^{-1} DW ASi), Gneiss and associated rock (class 2: 4.11±1.24 mg g^{-1} DW ASi), Sandstone and associated rock (class 9: 2.01±0.24 mg g^{-1} DW ASi. class 10: 2.06±0.01 mg g^{-1} DW ASi). ASi concentrations were lowest in Limestone (class 3: 0.03±0 mg g^{-1} DW ASi) (Fig. 2).
- Available **Si concentrations** were highest in Limestone and associated rock including shale (class 4: 5.65±0.78 mg g^{-1} DW Si), Quartz sandstone (class 6: 6.61±1.83 mg g^{-1} DW Si) and Sandstone (class 7: 5.46±0.66 mg g^{-1} DW Si). Si concentrations were lowest in Limestone and associated rock (class 3: 0.1±0.02 mg g^{-1} DW Si) (Fig. 2). Differences in available Si concentrations in the two classes of Limestone is mainly driven by the presence of shale in one class of the Limestone that acts as source for silicic acid.
- The highest available **Ca concentrations** were observed in Limestone (which consist of $CaCO_3$) and associated rock (class 3: 10.73±2.15 mg g^{-1} DW Ca), Sedimentary and/or volcanic rock (class 12: 8.77±0.12 mg g^{-1} DW Ca) and Sandstone and associated rock (class 8: 8.06±0.36 mg g^{-1} DW Ca). Ca concentrations were lowest in Gneiss (class 2: 0.05±0.02 mg g^{-1} DW Ca) (Fig. 2). The data consists with the expectations of highest Ca availability in Ca containing bedrock.
- Available **Fe concentrations** were highest in shale and associated rock (class 13: 2.93±0.45 mg g^{-1} DW Fe), Limestone (class 4: 2.28±0.32 mg g^{-1} DW Fe) and Quartz sandstone (class 6: 2.49±0.69 mg g^{-1} DW Fe). The lowest Fe concentrations were observed in lithological Limestone and associated rock (class 3: 0.01±0.001 mg g^{-1} DW Fe) (Fig. 2).
- The highest available **concentrations of Al** were observed in to quartz sandstone (class 6: 2.52±0.70 mg g^{-1} DW Al), Sandstone (class 7: 1.63±0.20 mg g^{-1} DW Al) and shale and associated rock (class 13: 1.5±0.23 mg g^{-1} DW Al). The lowest Al concentrations were observed in limestone and associated rock (class 3: 0.02±0 mg g^{-1} DW Al) (Fig. 2).
- High available **P concentrations** were observed in limestone and associated rock (class 4: 0.31±0.04 mg g^{-1} DW P), Sandstone (class 7: 0.19±0.02 mg g^{-1} DW P) and Shale and associated rock (class 14: 0.15±0.05 mg g^{-1} DW P). P concentrations were lowest in Basalt and associated rock (class 1: 0.0116±0.002 mg g-1 DW P) (Fig. 2).

Gelöscht: Limestone

Gelöscht: Sandstone

Gelöscht: fit

Gelöscht: being highest

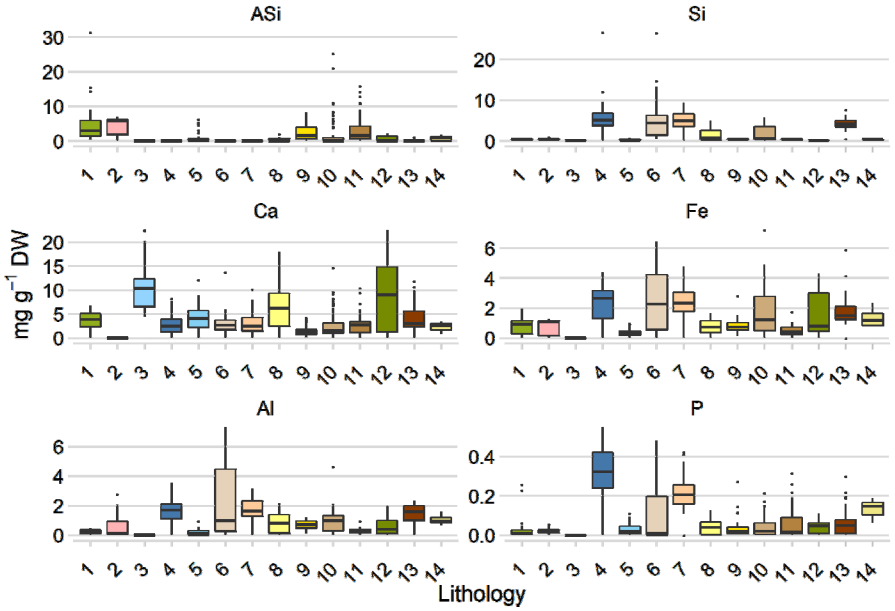

Fig. 2: Element concentrations related to lithology. Lithology 1 is igneous, class 2 is metamorphic and the rest are sedimentary, or sedimentary and mixed. Each color represents a bedrock lithology: 1: Basalt, olivine basalt, tholeiite, alkali basalt, basanite, pillow basalt, flood basalt (n=26); 2: Gneiss, migmatite; reworked amphibolite and granulite facies rocks (n=11); 3: Limestone, dolostone, shale, evaporites, chalk; carbonate reefs or metamorphosed equivalent (n=24); 4: Limestone, dolostone, shale, evaporites, chalk; carbonate reefs; metamorphic grade not identified (n=58); 5: Limestone, dolostone, shale, evaporites, chalk; carbonate reefs (n=64); 6: Quartz sandstone, siltstone, claystone, limestone, dolostone, conglomerate, tillite (n=13); 7: Sandstone, siltstone, shale, coal; plant fossils; metamorphic grade not identified (n=68); 8: Sandstone, siltstone, shale, limestone (n=38); 9: Sandstone, siltstone, shale, limestone; metamorphic grade not identified (n=39); 10: Sandstone, siltstone, shale; marine fossils (n=91); 11: Sandstone, siltstone, shale; marine fossils; metamorphic grade not identified (n=60); 12: Sedimentary and/or volcanic rock: undivided (n=21); 13: Shale, chert, iron-formation, greywacke, turbidite, argillaceous limestone, matrix-supported conglomerate (n=43); 14: Shale, chert, iron-formation, greywacke, turbidite, argillaceous limestone, matrix-supported conglomerate or metamorphosed equivalent (n=8). All values are given in mean and standard error. The distribution of the lithological classes is shown in Fig. 1, the assignment to the geographic domain is given in Table S5.

Gelöscht: color

Gelöscht: ¶

3.3 Maps of element concentration in 1 m depth

3.3.1 Amorphous silicon in top 1 m

- We found the highest concentrations of ASi located in the Arctic-North Atlantic region (Fig. 3). Here, basalt and Gneiss are dominant (lithological class 1 and 2) and contained concentrations of 4.11 ± 1.24 to 6.68±1.17 mg ASi g^{-1} DW. Other high concentrations of ASi were found for the Brooks Range (Alaska), Chukotka, Arctic Shelf (eastern Siberia) and the West Siberian Basin. Those soil contained 2.01 ± 0.24 mg ASi g^{-1} DW (lithological class 9). The Verkhoyansk-Kolyma region showed a lower concentration of 1.48 ± 0.16 mg ASi g^{-1} DW (lithological class 11). We found similar concentrations (1.24 ± 0.14 mg ASi g^{-1} DW; lithological class 5) for the Canadian Shield. We found low concentrations of 0.31± ± 0.01 mg ASi g^{-1} DW (lithological class 12) in interior western Alaska and western parts of Brooks Range, Alaska, Chukotka and Arctic Shelf. Increasing active layer depth will potentially release higher ASi concentrations from permafrost soils (Fig. S6) in the Canadian Shield as the concentration in the permafrost layer is 2.80 ± 2.50 mg ASi g^{-1} DW (lithological class 5) compared to the 1.24 ± 0.14 mg ASi g^{-1} DW in the current active layer (Table S4). A further increase in ASi concentration can be expected for the Arctic, North-Atlantic region by permafrost thaw as the concentration is 8.68 ± 2.51 mg ASi g^{-1} DW in the permafrost layer compared to the 4.11 ± 1.24 mg ASi g^{-1} DW of the current active layer (lithological class 1) (Fig. S6 Table S4). However, the permafrost layer in Siberia contains lower concentrations of ASi (0.77 ± 0.23 mg ASi g^{-1} DW, lithological class 9 and 1.38 ± 0.28 mg ASi g^{-1} DW, lithological class 11) compared to the current active layer with 2.01 ± 0.24 mg ASi g^{-1} DW (lithological class 9) and 1.48 ± 0.16 mg ASi g^{-1} DW (lithological class 11) probably leading to lower overall ASi concentrations with proceeding thaw. The variability of the ASi data is high for the lithological class 1, 2, 9 and 11.

Gelöscht: silica

Gelöscht: mafic

Gelöscht: metamorphic

Gelöscht: ±

Gelöscht: ±

Gelöscht: ±

Gelöscht: were found

Gelöscht: ±

Gelöscht: ±

Gelöscht: ±

Gelöscht: ±

Gelöscht: ±

Gelöscht: ±

Gelöscht: ±

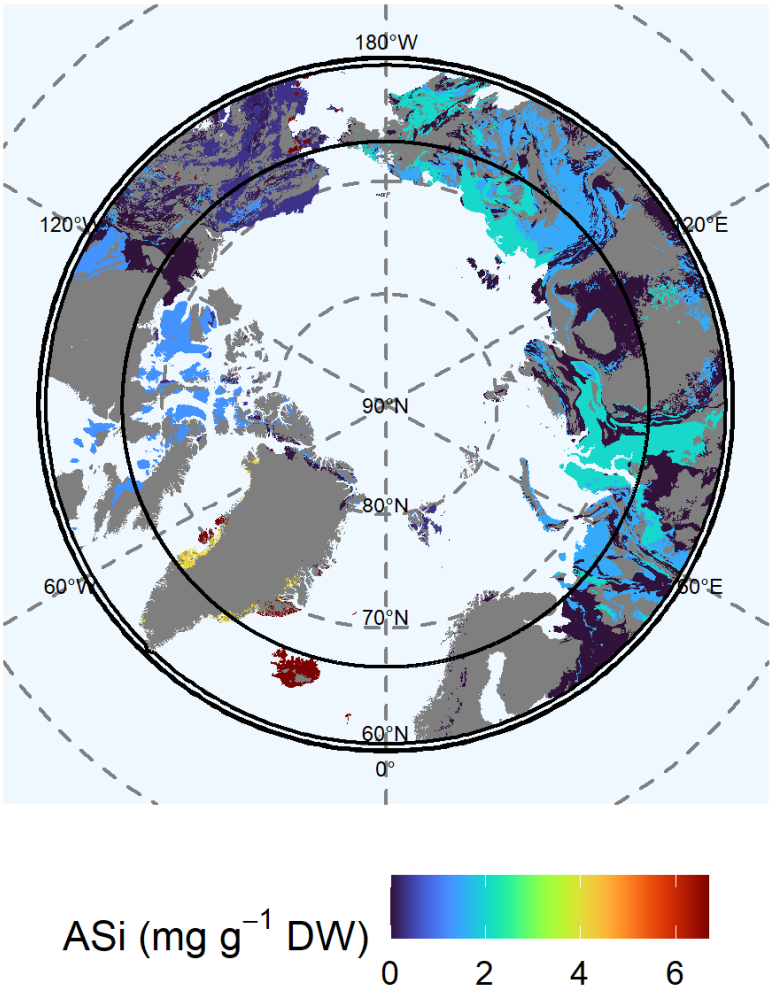

Fig. 3: Map of mean concentration of amorphous silicon (ASi) in the top 100 cm of soils. For each lithological class the mean concentration is shown. Grey shaded areas are not represented by our data.

Gelöscht: silica

3.3.2 Silicon in 0-1 m depth

Available Si (Mehlich III extractable) (Fig. 4), extracted as silicic acid, showed a different distribution than the solid fraction of ASi (Fig. 3). High available Si concentrations were generally associated with sediments. The available Si extracted by the Mehlich III extraction is water soluble Si plus Si bound to the surface of soil particles (Schaller et al., 2021). We found high concentrations (5.65 ± 0.78 mg Si g^{-1} DW) for lithological class 4, the West Siberian basin and the Siberian plain. Other regions with high available Si concentrations were the East European plain, the Ural Mountains and the Canadian Shield. Another lithological class with high available Si concentrations (4.51 ± 0.69 mg Si g^{-1} DW) is class 13, located in the Innutian Region, North Greenland and in Alaska. In Alaska lithological class 10 with moderate high concentrations of available Si (2.06 ± 0.03 mg Si g^{-1} DW) is also abundant. We found low concentration of available Si (0.36 ± 0.05 mg Si g^{-1} DW, lithological class 9) for Brooks Range, Chukotka, Arctic shelf, the West Siberia Basin and the Siberian Plain. In addition, the Verkhoyansk-Kolyma-Region and the East-European Plain and the Ural Mountains were poor in available Si (0.39 ± 0.04 mg Si g^{-1} DW, lithological class 11). Lowest available concentrations (0.15 ± 0.01 mg Si g^{-1} DW, lithological class 12) were observed in Interior Western Alaska. Increasing thawing depth may potentially increase available Si concentrations in the western Verkhoyansk-Kolyma-Region to the east European Platform as the concentration in the permafrost layer is 6.26 ± 1.52 mg Si g^{-1} DW (lithological class 4) compared to the lower available Si concentration of the current active layer with 5.56 ± 0.78 mg Si g^{-1}DW (lithological class 4) (Figure S6, Table S4). The variability of the data of available Si is high for the lithological class 4, 6 and 7.

Gelöscht: ±

Gelöscht: ±

Gelöscht: ±

Gelöscht: ±

Gelöscht: ±

Gelöscht: ±

Gelöscht: ±

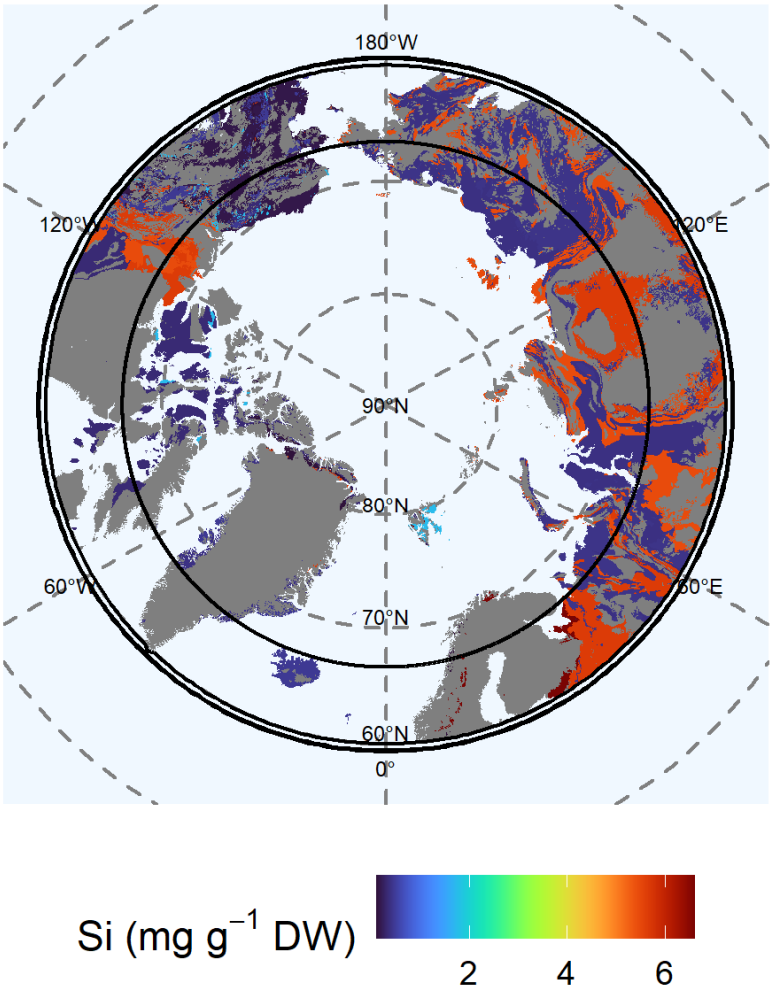

Fig. 4: Map of mean concentration of available silicon (Si) (Mehlich III extractable) for the uppermost 100 cm of soils. For each lithological class the mean concentration is shown. Blue colors represent low concentrations of available Si; red colors represent high concentrations. Grey shaded areas are not represented by our data.

Gelöscht: mineral

Gelöscht:

3.3.3 Calcium in 0-1m depth

The highest available Ca concentrations (Mehlich III extractable) in soils was in limestone and associated rock (class 3: 10.73 ± 2.15 mg Ca g^{-1} DW) in North Greenland, Alaska and the Canadian Shield (3.79 ± 0.45 mg Ca g^{-1} DW, lithological class 5) (Fig. 5). Particular limestone shows a high solubility under acidic conditions used in the Mehlich III extraction and by this shows high available Ca concentrations. In addition, supracrustal rocks in Alaska contained very high available concentrations of Ca (8.77 ± 0.12 mg Ca g^{-1} DW, lithological class 12). Mafic rocks in the Arctic North Atlantic region (3.65 ± 0.70 mg Ca g^{-1} DW, lithological class 1) contained moderate available Ca concentrations. We found moderate to low available Ca concentrations (2.88 ± 0.32mg Ca g^{-1} DW, lithological class 11) for the soils of the Verkhoyansk-Kolyma-Region, the East European Plain and the Ural Mountains. Large regions of eastern and western Siberia and the Siberian Plain were poor in available Ca (1.51 ± 0.14 mg Ca g^{-1} DW, lithological class 9; 2.56 ± 0.34 mg Ca g^{-1} DW, lithological class 4). The available Ca concentrations of the permafrost layer for Alaska (10.42 ± 2.08 mg Ca g-1 DW, lithological class 12) is higher than in the active layer (2.93 ± 0.45 mg Ca g^{-1} DW) (Fig. S6). In the largest part of Siberia and the Canadian Shield the available Ca concentrations are slightly lower in the permafrost layer with 2.15 ± 0.96 mg Ca g^{-1} DW (lithological class 4) and 1.59 ± 0.32 mg Ca g^{-1} DW, lithological class 7) than in the active layer with 2.56 ± 0.34 mg Ca g^{-1} DW (lithological class 4) and 1.51 ± 0.14 mg Ca g^{-1} DW, lithological class 7) (Figure S6, Table S4). The variability of the data of available Ca is high for the lithological class 1, 3, 5 and 6.

Gelöscht: ±
Gelöscht: ±
Gelöscht: In p
Gelöscht: leads
Gelöscht: to a
Gelöscht: ±
Gelöscht: c
Gelöscht: ±
Gelöscht: ±
Gelöscht: ±
Gelöscht: ±
Gelöscht: ±
Gelöscht: ±
Gelöscht: ±
Gelöscht: ±
Gelöscht: ±
Gelöscht: ±

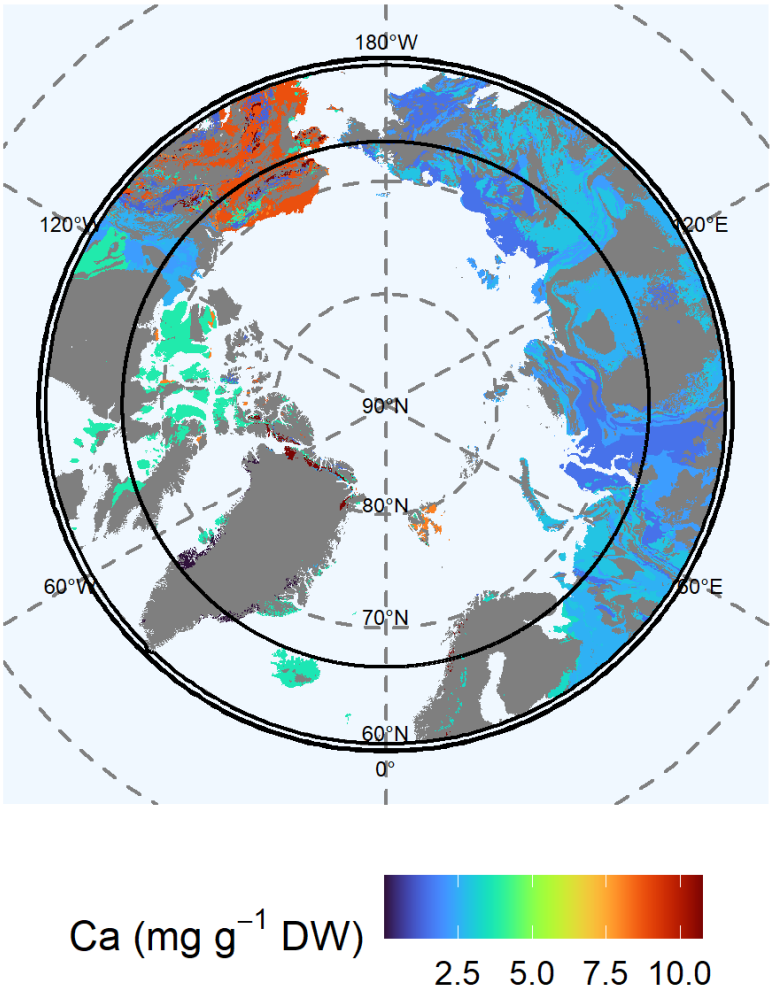

519

520 Fig. 5: Map of mean concentration of available calcium (Ca) (Mehlich III extractable) for the uppermost 100 cm of
521 soils. For each lithological class the mean concentration is shown. Blue colors represent low concentrations of Ca, red
522 colors represent high concentrations. Grey shaded areas are not represented by our data.

523

Gelöscht: mineral

Gelöscht:

3.3.4 Iron (Fe) in 0-1 m depth

Available Fe concentrations (Mehlich III extractable) were higher in the eastern Arctic, than in the western Arctic (Fig. 6). We found highest concentrations in northern Greenland (lithological class 13 contained 2.93 ± 0.45 mg Fe g^{-1} DW). The soils of the lithological class 4 in the western Siberian Basin, Siberian and Canadian plain contained 2.28 ± 0.32 mg Fe g^{-1} DW. The Verkhoyansk-Kolyma region showed similar Fe concentrations (2.21 ± 0.27 mg Fe g^{-1} DW, lithological class 7). Moderate to high Fe concentration we found for igneous mafic rocks in Iceland and Greenland (0.94 ± 0.18 mg Fe g^{-1} DW, lithological class 1) and for supracrustal rocks in Alaska (1.24 ± 0.14 mg Fe g^{-1} DW, lithological class 12). The Chukotka region and western Siberia were relatively poor in Fe (0.83 ± 0.13 mg Fe g^{-1} DW, lithological class 9). Eastern Siberia and North Europe contained even lower Fe concentrations (0.49 ± 0.04 mg Fe g^{-1} DW, lithological class 11). Available Fe concentrations in the Canadian Shield were similarly low (0.41 ± 0.06 mg Fe g^{-1} DW, lithological class 12). We expect increasing Fe concentrations at the Canada and Greenland shield due to predicted future thaw of the permafrost layer as the concentration in the permafrost layer (0.61 ± 0.15 mg Fe g^{-1} DW, lithological class 5) and in parts of Alaska (1.97 ± 0.3 mg Fe g^{-1} DW, lithological class 14) is higher compared to the current active layer with (0.41 ± 0.05 mg Fe g^{-1} DW, lithological class 5) and in parts of Alaska (1.08 ± 0.38 mg Fe g^{-1} DW, lithological class 14) (Fig. S7, Table S4). The variability of the data of available Fe is high for the lithological class 2 and 6.

Gelöscht: ±
Gelöscht:
Gelöscht:
Gelöscht:
Gelöscht: 21
Gelöscht: ±
Gelöscht:
Gelöscht: ±
Gelöscht:
Gelöscht:
Gelöscht: ±
Gelöscht: ±
Gelöscht: Fe
Gelöscht: ±
Gelöscht: ±
Gelöscht: ±
Gelöscht: ±
Gelöscht: ±

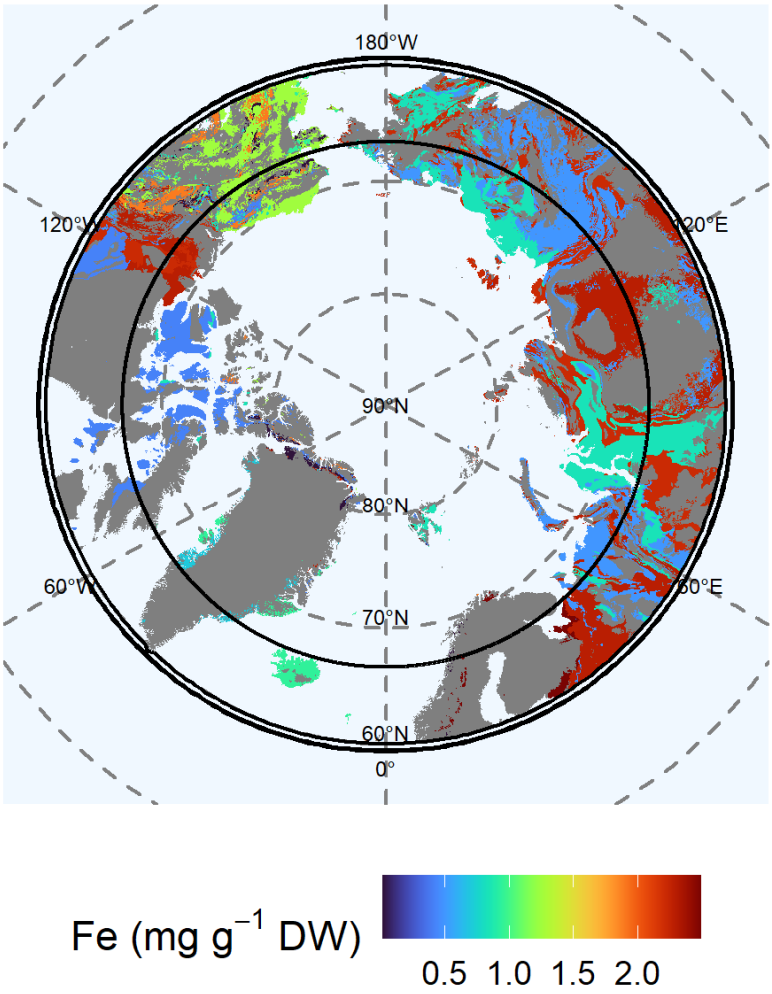

Fig. 6: Map of mean concentration of available iron (Fe) (Mehlich III extractable) for the uppermost 100 cm of soils. For each lithological class the mean concentration is shown. Blue colors represent low concentrations of Fe, red colors represent high concentrations Grey shaded areas are not represented by our data.

Gelöscht: mineral

Gelöscht:

3.3.5 Aluminum in 0-1 m depth

Northern Europe contained highest concentrations of available Al (Mehlich III extractable) (2.52 ± 0.7 mg Al g^{-1} DW, lithological class 6) (Fig. 7). Relative high concentrations of available Al were distributed over Siberia and the Canadian Shield (1.63 ± 0.02 mg Al g^{-1} DW, lithological class 7; 1.57 ± 0.22 mg Al g^{-1} DW lithological class 4). Parts of Alaska contained moderate available Al concentrations (0.94 ± 0.06 mg Al g^{-1} DW, lithological class 10; 1.5 ± 0.23 mg Al g^{-1} DW, lithological class 13), while areas represented by supracrustal rocks were poor in available Al (0.47 ± 0.06 mg Al g^{-1} DW, lithological class 12). We found relative low concentrations (0.73 ± 0.01 mg g-1 DW) of available Al for Chukotka, eastern and western Siberia observed in lithological class 9. The Verkhoyansk-Kolyma Region and the East European plain showed the lowest available Al concentrations (0.26 ± 0.02 mg Al g^{-1} DW, lithological class 11), together with the Canada plain (0.21 ± 0.03 mg g^{-1} DW Al, lithological class 5). Increasing thawing depth may increase the available Al concentration by the predicted thaw of the permafrost layer in North Europe as the concentration in the permafrost layer is 4.88 ± 1.02 mg Al g^{-1} DW (lithological class 6) and across the Greenland and Canadian shield it is 0.3 ± 0.07 mg Al g^{-1} DW (lithological class 5) compared to the current active layer with 2.52 ± 0.7 mg Al g^{-1} DW (lithological class 6) and across the Greenland and Canadian shield it is 0.21 ± 0.03 mg Al g^{-1} DW (lithological class 5) (Fig. S7, Table S4). The variability of the data of available Al is high for the lithological class 2 and 6.

Gelöscht: ±
Gelöscht: 0
Gelöscht: ±
Gelöscht: ±
Gelöscht: ±
Gelöscht: ±
Gelöscht: ±
Gelöscht: ±
Gelöscht: ±
Gelöscht: ±
Gelöscht: ±
Gelöscht: ±
Gelöscht: ±

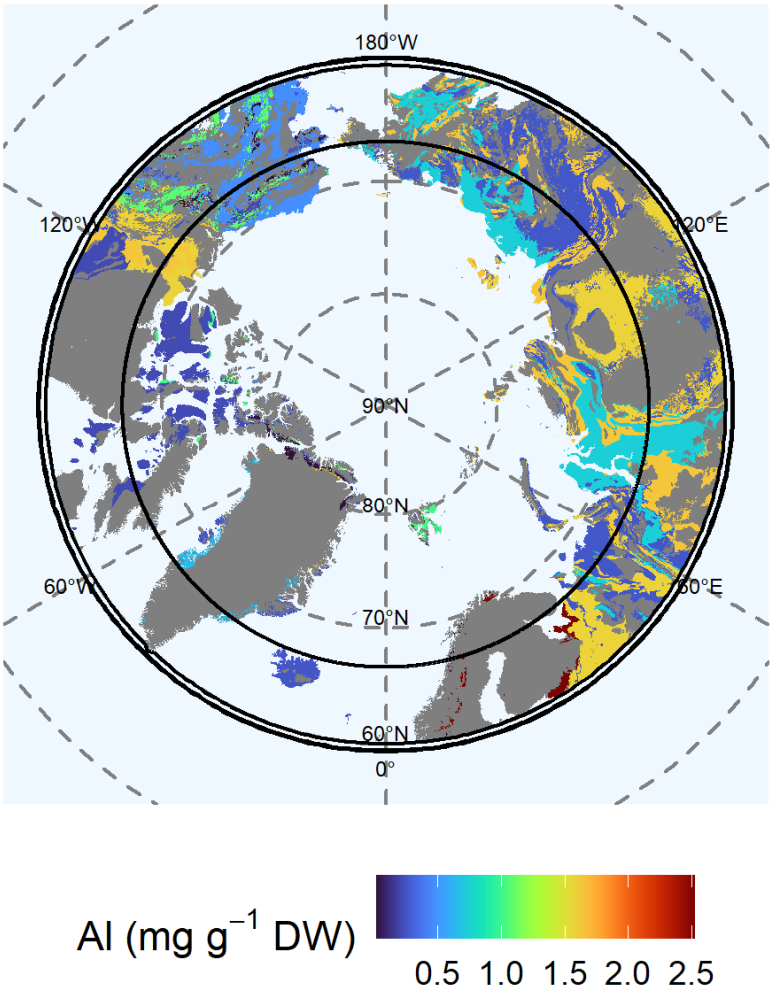

596

597 Fig. 7: Map of mean concentration of available aluminium (Al) (Mehlich III extractable) for the uppermost 100 cm of
598 soils. For each lithological class the mean concentration is shown. Blue colors represent low concentrations of Al, red
599 colors represent high concentrations. Grey shaded areas are not represented by our data .

Gelöscht: mineral aluminum

Gelöscht:

3.3.6 Phosphorous in 0-1 m depth

We found the highest available P concentrations (Mehlich III extractable) we found for the West Siberian Basin, the Canadian Shield and the Siberian and East European Plain (0.306 ± 0.042 mg P g^{-1} DW, lithological class 4) (Fig. 8). In the Chukotka region the available P concentrations were 0.189 ± 0.023 mg P g^{-1} DW (lithological class 7. We found moderate available P concentration for Northern Europe (0.123 ± 0.034 mg P g^{-1} DW, lithological class 6) and in Alaska (0.153 ± 0.054 mg P g^{-1} DW, lithological class 14). Wide areas of supracrustal rocks in Alaska were poor in available P (0.024 ± 0.004 mg P g^{-1} DW, lithological class 12). The Canadian shield (0.037 ± 0.005 mg P g^{-1} DW, lithological class 5), the Verkhoyansk-Kolyma region, the east European Plain (0.017 ± 0.002 mg P g^{-1} DW, lithological class 11) and the Chukotka region (0.030 ± 0.003 mg P g^{-1} DW, lithological class 9) were poor in P. Due to permafrost thaw we expect increasing available P concentrations the Canadian shield as the available P concentrations in the permafrost layer is 0.06 ± 0.01 mg P g^{-1} DW (lithological class 5) compared to the current active layer with 0.04 ± 0.005 mg P g^{-1} DW (lithological class 5) (Fig. 7, Table S4). The variability of the data of available P is high for the lithological class 4, 6 and 7.

Gelöscht: ±
Gelöscht: ±
Gelöscht: ±
Gelöscht: ±
Gelöscht: ±
Gelöscht: ±
Gelöscht: ±
Gelöscht: ±
Gelöscht: ±
Gelöscht: ±

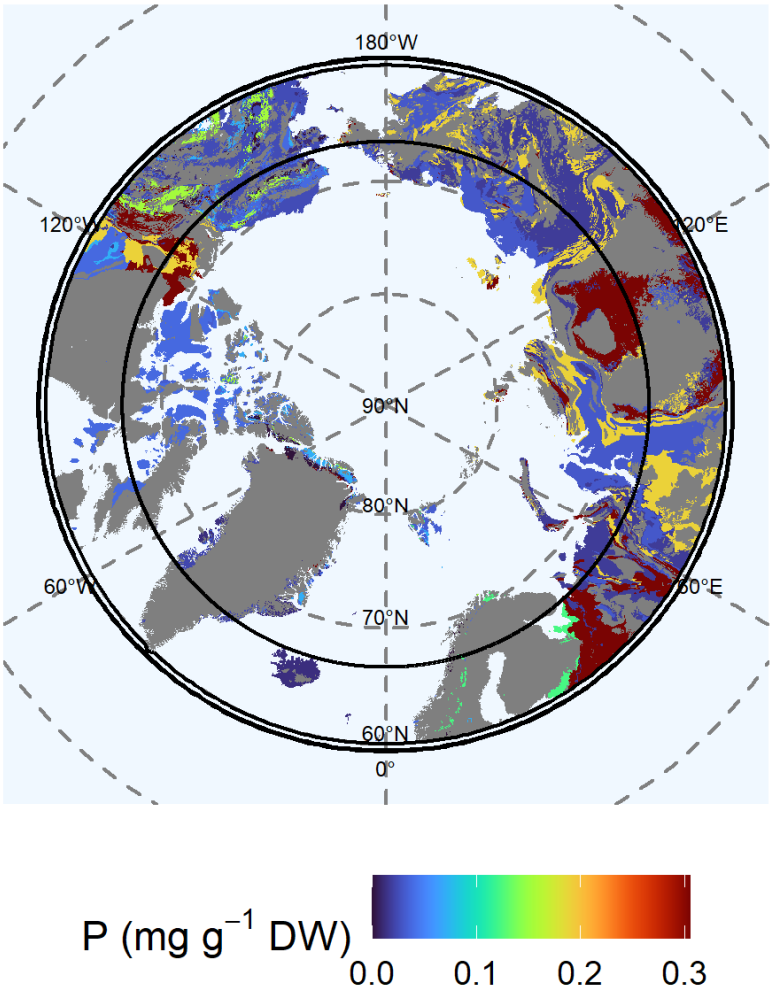

Fig. 8: Map of mean concentration of available phosphorous (P) (Mehlich III extractable) for the uppermost 100 cm of soils. For each lithological class the mean concentration is shown. Blue colors represent low concentrations of P, red colors represent high concentrations. Grey shaded areas are not represented by our data .

Gelöscht: mineral

Gelöscht:

4 Discussion

4.1 Element availability in relation to lithology and geography

We found large differences in the availability of all analysed elements between the different lithology classes of the Arctic. The igneous lithological type for example is dominated by alkaline and Ca-rich basaltic rocks from Alaska. Sedimentary rocks covers a wide range of pH, as sediments of diverse origin can contribute to form a sedimentary rock (Schirrmeister et al., 2011). In regions with fluvial deposition, e.g. in Yedoma affected areas, the soil forming material may differ from the underlying bedrock (Kokelj et al., 2017). Limestone sediments for example differ in their content of available Fe and P, depending if their origin is biological (lithological class 4), physical or chemical. Sandstone can contain high available Fe concentrations, too, but it contains available Si as the main element (lithological class 7-8) (Yurchenko et al., 2019). Previously, there was no map existing for availability of Si, Ca, Fe, P, and Al in Arctic soils, and only a map on ASi stocks but not concentrations. Our maps show element concentration available for plants and microbes together. We further show potential changes in element availability by deepening of the active layer, element export by run-off from thawed soil and thermokarst processes.

4.2 Relevance of element availability in a dynamic Arctic

Nutrient cycles and limitations were identified as important for improving of high latitude ecosystems estimations vegetation functional parameter like gross primary production (GPP) (Chadburn et al., 2017). The dataset presented in our study could therefore serve as a basis for providing soil nutrient concentrations for biogeochemical models that are capable of considering nutrient limitations in permafrost ecosystems. Our maps cover nearly the half of the Arctic area. The distribution of ASi in Arctic regions was first estimated by (Alfredsson et al., 2016). Alfredsson et al.(2016) showed maps of ASi stocks (not concentrations) related to vegetation cover, covering 30 soil profiles. Elements like Si and Ca are accumulated by plants, depending on the vegetation type (Jobbágy and Jackson, 2001; Mauclet et al., 2022). By this the effect of current vegetation on element availability in soils is associated with high uncertainties as the vegetation involved in forming the soil ASi pool may be different from the current vegetation (Andreev Andrei A. et al., 2003; ANDREEV et al., 2016; Schweger, 1982). A more appropriate measure of element availability may be parent material and lithology (Alloway, 2013). It was shown, that geochemical element concentration in Arctic permafrost soil allow to distinguish geologies (Reimann and Melezhik, 2001). Consequently, our lithology-based extrapolation of nutrient availability will help to reduce the so far uncertainties in pan-Arctic soil element availability. Due to deepening of the active layer, as for example at the Canadian Shield and in the North-Atlantic region, our data suggest higher ASi concentrations in the active layer in future, as the concentration in the permafrost layer is higher compared to current active layer (Fig. S6). This higher ASi concentrations may increase P and OM availability (Reithmaier et al., 2017; Schaller et al., 2019) by polysilicic acid competing for binding sites on the surface of minerals subsequently mobilizing both P and OM as ASi is a main source for polysilicic acid, potentially increasing the leaching of both elements to the sea. It was also shown that available Si leads to a release of P from minerals of Arctic soils and increases OM decomposition, increasing soil greenhouse gas release (Schaller et al., 2019; Schaller et al., 2021b).

Gelöscht: ¶

Gelöscht: ¶

Gelöscht:

Gelöscht: Rocks built up by sedimentation are often more complex or variable in their chemical composition than igneous rocks.

Gelöscht: Sedimentary rocks covers a wide range of pH, as

Gelöscht: the parent material is more diverse

Gelöscht: generating

Gelöscht: can

Gelöscht: what

Gelöscht: will occur during

Gelöscht: permafrost thaw

Gelöscht: and we discuss these changes in element availability in regard to occurring nutrient limitations and Arctic C-fluxes

Gelöscht: .

Gelöscht: Low temperatures in the Arctic systems slow down biological and chemical processes and preserve OM for millennia (Sher et al., 2005). Due to Arctic warming these processes are accelerated by an increased nutrient and OM mobilization from the permafrost (Salmon et al., 2016). Consequently, OM may become vulnerable to respiration (Hugelius et al., 2020; Strauss et al., 2017). However, OM is not the single driving force regarding the acceleration of Arctic soil respiration. Available eElements like Si, Ca, Fe, P and Al may also interfere this process (Monhonval et al., 2021a; Monhonval et al., 2021b). ¶

Gelöscht: (

Gelöscht: T

Gelöscht: mineral

Gelöscht: low and

Gelöscht: observed

Gelöscht: shield

Gelöscht: shallower

Gelöscht: soil layers

Feldfunktion geändert

Formatiert: Englisch (Großbritannien)

Formatiert: Englisch (Großbritannien)

Available Ca can immobilize OM by cation bridging and by this preserve OM from microbial decomposition (Sowers et al., 2020). Available Ca is relevant for the mineral formation because it can bind CO_2 as $Ca(HCO_3)_2$ in soil with pH higher than 7 (Dessert et al., 2003; Köhler et al., 2010). The concentration of soluble Ca in Yedoma soils is mainly driven by thermokarst processes (Monhonval et al., 2022). In permafrost layers, the data presented in Fig. S6 shows Ca concentrations are in most locations lower than in the current active layers, which is in accordance to other studies (Kokelj and Burn, 2005). Consequently, a future increase in temperatures may lead to a widespread decrease in available Ca concentrations in average at 0-1 m depth, especially in the Yedoma regions. Iron minerals are important electron acceptors under anaerobic conditions and available Fe is essential forko microbial methane production (Colombo et al., 2018). After being released from rocks by weathering, Al forms amorphous aluminosilicates that crystalize slowly (Schaller et al., 2021a). The Mehlich III extract contains all soluble forms of $Al(OH)(H_2O)$ that are bioavailable for organisms, with Al being toxic (Rengel, 2004). Thawing permafrost may be a source for available Al, especially across Canada, the Greenland shield and Northern Europe. Increasing P availability, as predicted for Greenland and the Canadian shield (Fig. 7) may for example increase CO_2 release to the atmosphere by increasing the mineralization rates of OM (Street et al., 2018; Yang and Kane, 2021).

4.3 Importance of element interactions for nutrient availability

In permafrost layers, the mineralization of OM by microbial activity is negligible due to frozen conditions. Like in temperate soils, binding of OM on mineral phases can prevent OM from mineralization (Dutta et al., 2006; Mueller et al., 2015). Mineral phases may bind parts of soil OM reducing the amount of OM for microbial respiration. A large share of OM may be associated with iron and aluminium oxides/hydroxides. In particular iron minerals may strongly bind OM, whereby a high stability of stored carbon is likely (Herndon et al., 2017). Thereby the binding between OM and the minerals is determined by the quantity of minerals that can bind OM (Wiseman and Püttmann, 2006). This would imply that a higher concentration of available Fe, Al and Ca in Arctic soils due to permafrost thaw may lead to a lower GHG emission from Arctic soils due to complexation of OM with those elements. Such increase in element availability binding OM and with this resulting in potentially lower GHG emissions may happen for Alaska (higher available Ca and available Fe concentration in permafrost layer compared to current active layer), Canadian Shield and Greenland (higher available Fe and available Al concentration in permafrost layer compared to current active layer), and North Europe (higher available Al concentration in permafrost layer compared to current active layer) (see results part). However, lower available Ca concentrations can be expected in large parts of Siberia and the Canadian Shield, as the concentrations in the permafrost layer are lower compared to the current active layer. Available silicon however, can potentially mobilize OM from those phases under slight acidic to alkaline and also from oxic to anoxic conditions, by binding competition of silicic acid with some functional groups of organic material (Hömberg et al., 2020), potentially increasing GHG emissions. An increase in Si availability upon permafrost thaw can be expected in the western Verkhoyansk-Kolyma-Region to the east European Platform as the concentration in the permafrost layer is higher compared to the current active layer (see results part). Available P competes with OM for binding on soil minerals (Schneider et al., 2010). Such increasing P concentration due to permafrost thaw can be expected for the

Gelöscht: Calcium

Gelöscht: Calcium reduces the osmotic stress for microbes (Läuchli and Grattan, 2007) by decreasing the freezing point of water and increasing the availability of liquid pore water (Jessen et al., 2014).

Gelöscht: deeper soil

Gelöscht: usually

Gelöscht: upper soil

Formatiert: Affiliation Char, Schriftfarbe: Automatisch

Gelöscht: In deeper soil layers, Ca concentrations are usually lower than in upper layers.

Gelöscht: Fe Iron is also of high importance for ecosystems as it is a key element in microbial activity (Colombo et al., 2014) and nitrogen fixation (Jasniewski et al., 2019).

Gelöscht: Fe

Gelöscht: silica

Gelöscht: mineralizes

Gelöscht: Aluminium extracted by

Gelöscht: is

Gelöscht: respiration

Gelöscht: due to its high cytotoxicity to

Feldfunktion geändert

Formatiert: Englisch (Großbritannien)

Gelöscht: S

Gelöscht: some

Canadian Shield (results part). Based on the differences in element (Si, Fe, Al, Ca and P) available concentration, the stability of OM differs in Arctic regions, depending on the dominating mineral composition, lithology and element availability. Also the availability of nutrients (P in this case) is modified by mineral composition. For example, P is often strongly bound to Fe mineral phases, reducing P availability (Gérard, 2016). Silicic acid, however, is able to mobilize P from strong binding to Fe mineral by competing for binding sites in a wide range of conditions (Schaller et al., 2019). Unlike Si, Ca binds P by calcium phosphate precipitation at alkaline conditions (Cao and Harris, 2008) or as calcium carbonate/phosphate co-precipitation (Otsuki and Wetzel, 1972). Under conditions of low Fe availability in soils, the binding of P may be related to Al-minerals (Eriksson et al., 2015). A lack of available P leads also to a reduction of the physiological activity of microbes (Walker et al., 2001), thus potentially reducing microbial respiration of OM. Mobile Si in forms of silicic acid and its polymers may potentially limit the availability of ions like Fe, Al, or Ca by precipitating those elements in amorphous or crystalline phases (Schaller et al., 2021a). Hence, the mobilization of elements like Si, Ca, Fe and Al strongly interfere with both P and OM availability and thus potentially with GHG emissions. To unravel the dominant processes upon permafrost thaw, or which element mobilization is dominant in terms of OM binding or mobilization and with this affecting GHG emission, future studies are urgently needed.

Gelöscht: on

Gelöscht: some

Gelöscht: Free

Gelöscht: seems

4.4 Transport of elements to the Arctic Ocean

With the ongoing deepening of the active layer in Arctic soils, an increased leaching of elements and nutrients may occur (Mann et al., 2022; Sanders et al., 2022), which may substantially impact marine biodiversity and ecosystem function. We have shown for several regions of the Arctic that there will be regional differences in element mobilization upon permafrost thaw. For example, increased export of Fe and P, which are the main limiting nutrients for marine net primary production (NPP); (Zabel and Schulz, 2006), has already contributed to a 30% increase in NPP in the Arctic Ocean between 1998 and 2009 (Arrigo and van Dijken, 2011). Increased available Fe concentrations at the depth of 0-1 m in the soils upon permafrost thaw can be expected for soils developed on the Canadian Shield, Greenland and Alaska, whereas increased P mobilization may occur only in the Canadian Shield, according to the sites studied within these lithological classes. Silicon and Ca also have a crucial role in marine primary production. Both elements are components of the inorganic spheres of diatoms (Si) and coccolithophores (Ca), which fix CO_2 in the Arctic Ocean, an important global carbon sink (Krause et al., 2018). At the Arctic Canadian coast, Si inputs led to an increase of diatoms from 2% to 37% (Terhaar et al., 2021). Diatoms and coccolithophores are the basis of the marine food chain, and therefore, shifts in their populations may have widespread implications for the marine ecosystem (Daniels et al., 2018). Permafrost thaw is likely to accelerate inputs of available Si and Ca to Arctic waters. Increased Si availability in soils can be expected in the western Verkhoyansk-Kolyma-Region to the east European Platform as the concentration in the permafrost layer is higher compared to the current active layer, (see Results section). Calcium mobilization may increase or decrease depending on the Arctic region. Increase Ca mobilization can be expected for Alaska, whereas a slight decrease in Ca mobilization may occur in large parts of Siberia and the Canadian Shield (see Results section). Yedoma deposits readily leach soluble ions, including Si and Ca, as a result of

Gelöscht: concentration

Gelöscht: availability

Gelöscht: concentration

thaw degradation (Strauss et al., 2017b). Alaskan soils store huge amounts of available Ca in the mineral layer (see above) that could be transported to the Beringia Sea with increasing soil degradation, promoting the growth of coccolithophores. In Siberia, the Lena River could transport large amounts of available Si to the Laptev Sea increasing the growth of diatoms. The same could happen at the East European plain. In the same way P concentrations in these regions of the Arctic Sea could rise, too, as P concentrations in the permafrost layer of the Canadian Shield are higher compared with the current active layer (see results part). During the transport to the ocean the elements may be bound to soil particles potentially decreasing the further transport or may interact with other elements (see paragraph before) also potentially affecting the further transport. In summary, in many areas of the Arctic with high available Si, Ca and P storage, there could be increased inputs to Arctic waters with permafrost thaw potentially increasing CO_2 fixation by marine primary production.

4.5. Limitations of data and statistics

Despite sample number of our study being quite high and reflecting a broad range of the pan-Arctic regions, this study has still some limitations. The density of data points is not homogeneous over the whole area and in some remote areas the sample number is low. To reduce potential uncertainties and variance in the presented data on available element concentrations we did bootstrapping for the single layers within the lithological classes. Our data does not give total element pools, but biological available concentrations.

5 Data availability

The data for element availability from all single locations, soil profiles, transects, lithology's, as well as bootstrap data for location and lithology can be can be downloaded via the open-access MPG repository EDMONT under https://doi.org/10.17617/3.8KGQUN (Schaller and Goeckede, 2022). During review process, the data is available under: https://edmond.mpdl.mpg.de/privateurl.xhtml?token=8cbb0bd8-790f-4719-8cd1-a3df4ff99477 to allow corrections based on reviewer comments (Schaller and Goeckede, 2022). The repository contains a readme file ("Read me.docx"). In this file, all necessary information can be found, including all columns descriptions need to use the data. The element availability from all single locations, soil profiles, transects, lithology's labelled (loction_samples.txt) with following parameters: geological map of the Arctic, individual ID of the polygon, official name of the sampling site, study internal name of the soil sample, soil horizon, coordinates of sampling sites, concentration of alkaline extractable amorphous silicon (ASi), Mehlich-3 extractable Si, Ca, Fe Al and P, thickness of the layer, original depth where soil was taken, size of the polygon that contains the sampling site, age code, scientific name of the age, where bedrock was formed, scientific name of the eon, where bedrock was formed, scientific name of the era, where bedrock was formed, scientific name of the period, where bedrock was formed, maximal and minimal age of bedrock, information if lithogenesis was of the supracrustal, sedimentary or igneous type, most common rock types in the cluster group of the setting, code of metamorphic type, code of domain region, name of tectonic and geographic domain, as well as name of region within geographic domain.

Gelöscht: the

Gelöscht: Even if the

Gelöscht: is

Gelöscht: s

Gelöscht: some

Gelöscht: have to be done

Gelöscht: the

Gelöscht: ,

In the location_bootstrap.txt file the bootstrapped means of concentration of alkaline extractable silicon, Mehlich-3 extractable Si, Ca, Fe Al and P for the organic, mineral active and permafrost layer of the single locations are given in mg/g DW.

In the file "lithology_bootstrap.txt" element concentration for the first 1 m, including organic, mineral and permafrost layer are given as bootstrapped mean with standard deviation for alkaline extractable silicon as well as Mehlich-3 extractable Si, Ca, Fe Al and P.

6 Conclusion

Here, we identified large differences in concentrations in available Si, Ca, Fe, P, Al and the solid ASi fraction between different Arctic regions. With the future projected warming of the Arctic and the associated thaw of permafrost soils by deepening the active layer, the available concentration of the elements will change, which will likely lead to difference in their availability according to our data. Depending on dominance or limitation of certain elements, biogeochemical processes such as OM mineralization may increase or decrease. Moreover, not only microbial processes like OM respiration may be affected by changes in Si, Ca, Fe, P, and Al availability, but also processes such as primary production (CO_2 fixation by plants) in terrestrial systems. This could be stabilizing soil OM, but may also trigger elevated biomass production of plants due to increased nutrient supply. In addition, marine systems will receive higher loads of leached elements, which could increase algae biomass production due to larger nutrient transport to the sea. Our spatially data product including the differences in elements availability between the different lithological classes and regions will help improving models of Arctic biogeochemical cycles for estimating future carbon feedback under the predicted climate change.

Gelöscht: and

Gelöscht: availability

Formatiert: Affiliation Char

Gelöscht: the availabilities of the elements will change

Competing interests. The contact author has declared that neither they nor their co-authors have any competing interests.

Acknowledgments. We thank Mrs. Lidia Völker (ZALF) for help with data extraction from the GIS polygons.

Financial support. The work was funded by the German Research Foundation (DFG), grant number SCHA 1822/12-1 to Jörg Schaller. J. Strauss work was embedded into the 'Changing Arctic Ocean (CAO)' program (CACOON project [#03F0806A (BMBF)]. Grant NSF-1417700 to SMN.

References

Abbott, B. W., Jones, J. B., Godsey, S. E., Larouche, J. R., and Bowden, W. B.: Patterns and persistence of hydrologic carbon and nutrient export from collapsing upland permafrost, Copernicus GmbH, 2015.

Alfredsson, H., Clymans, W., Hugelius, G., Kuhry, P., and Conley, D. J.: Estimated storage of amorphous silica in soils of the circum-Arctic tundra region, Global Biogeochem. Cycles, 30, 479–500, https://doi.org/10.1002/2015GB005344, 2016.

Alloway, B. J.: Bioavailability of Elements in Soil, in: Essentials of Medical Geology, edited by: Selinus, O., Springer, Dordrecht, 351–373, https://doi.org/10.1007/978-94-007-4375-5_15, 2013.

ANDREEV, A. A., TARASOV, P. E., Wennrich, V., and MELLES, M.: Millennial-scale vegetation changes in the north-eastern Russian Arctic during the Pliocene/Pleistocene transition (2.7–2.5 Ma) inferred from the pollen record of Lake El'gygytgyn, Quaternary Science Reviews, 147, 245–258, https://doi.org/10.1016/j.quascirev.2016.03.030, 2016.

Andreev Andrei A., TARASOV, P. E., ARASOV, P. E., Siegert, C., EBEL, T., KLIMANOV, V. A., MELLES, M., BOBROV, A. A., DEREVIAGIN, A. Y., LUBINSKI, D. J., and Hubberten, H.-W.: Late Pleistocene and Holocene vegetation and climate on the northern Taymyr Peninsula, Arctic Russia, Boreas, 32, 484–505, https://doi.org/10.1080/03009480310003388, 2003.

Arrigo, K. R. and van Dijken, G. L.: Secular trends in Arctic Ocean net primary production, J. Geophys. Res., 116, 1–15, https://doi.org/10.1029/2011JC007151, 2011.

Box, J. E., Colgan, W. T., Christensen, T. R., Schmidt, N. M., Lund, M., Parmentier, F.-J. W., Brown, R., Bhatt, U. S., Euskirchen, E. S., Romanovsky, V. E., Walsh, J. E., Overland, J. E., Wang, M., Corell, R. W., Meier, W. N., Wouters, B., Mernild, S., Mård, J., Pawlak, J., and Olsen, M. S.: Key indicators of Arctic climate change: 1971–2017, Environ. Res. Lett., 14, 45010, https://doi.org/10.1088/1748-9326/aafc1b, available at: https://iopscience.iop.org/article/10.1088/1748-9326/aafc1b/meta, 2019.

Brown, J. and Romanovsky, V. E.: Report from the International Permafrost Association: state of permafrost in the first decade of the 21st century, Permafrost Periglac. Process., 19, 255–260, https://doi.org/10.1002/ppp.618, 2008.

Cao, X. and Harris, W.: Carbonate and magnesium interactive effect on calcium phosphate precipitation, Environmental science & technology, 42, 436–442, https://doi.org/10.1021/es0716709, 2008.

Chadburn, S. E., Krinner, G., Porada, P., Bartsch, A., Beer, C., Belelli Marchesini, L., Boike, J., Ekici, A., Elberling, B., Friborg, T., Hugelius, G., Johansson, M., Kuhry, P., Kutzbach, L., Langer, M., Lund, M., Parmentier, F.-J. W., Peng, S., van Huissteden, K., Wang, T., Westermann, S., Zhu, D., and Burke, E. J.: Carbon stocks and fluxes in the high latitudes: using site-level data to evaluate Earth system models, Biogeosciences, 14, 5143–5169, https://doi.org/10.5194/bg-14-5143-2017, 2017.

Colombo, N., Salerno, F., Gruber, S., Freppaz, M., Williams, M., Fratianni, S., and Giardino, M.: Review: Impacts of permafrost degradation on inorganic chemistry of surface fresh water, Global and Planetary Change, 162, 69–83, https://doi.org/10.1016/j.gloplacha.2017.11.017, 2018.

Daniels, C. J., Poulton, A. J., Balch, W. M., Marañón, E., Adey, T., Bowler, B. C., Cermeño, P., Charalampopoulou, A., Crawford, D. W., Drapeau, D., Feng, Y., Fernández, A., Fernández,

Formatiert: Englisch (Großbritannien)

E., Fragoso, G. M., González, N., Graziano, L. M., Heslop, R., Holligan, P. M., Hopkins, J., Huete-Ortega, M., Hutchins, D. A., Lam, P. J., Lipsen, M. S., López-Sandoval, D. C., Loucaides, S., Marchetti, A., Mayers, K. M. J., Rees, A. P., Sobrino, C., Tynan, E., and Tyrrell, T.: A global compilation of coccolithophore calcification rates, Earth Syst. Sci. Data, 10, 1859–1876, https://doi.org/10.5194/essd-10-1859-2018, 2018.

DeMaster, D. J.: The supply and accumulation of silica in the marine environment, Geochimica et Cosmochimica Acta, 1715–1732, 1981.

Dessert, C., Dupré, B., Gaillardet, J., François, L. M., and Allègre, C. J.: Basalt weathering laws and the impact of basalt weathering on the global carbon cycle, Chemical Geology, 202, 257–273, https://doi.org/10.1016/j.chemgeo.2002.10.001, 2003.

Dutta, Schuur, E. A. G., Neff., and Zimov, S. A.: Potential carbon release from permafrost soils of Northeastern Siberia, Global change biology, 12, 2336–2351, https://doi.org/10.1111/j.1365-2486.2006.01259.x, 2006.

Eriksson, A. K., Gustafsson, J. P., and Hesterberg, D.: Phosphorus speciation of clay fractions from long-term fertility experiments in Sweden, Geoderma, 241-242, 68–74, https://doi.org/10.1016/j.geoderma.2014.10.023, 2015.

Faucherre, S., Jørgensen, C. J., Blok, D., Weiss, N., Siewert, M. B., Bang-Andreasen, T., Hugelius, G., Kuhry, P., and Elberling, B.: Short and Long-Term Controls on Active Layer and Permafrost Carbon Turnover Across the Arctic, J. Geophys. Res. Biogeosci., 123, 372–390, https://doi.org/10.1002/2017JG004069, 2018.

Fuchs, M., Grosse, G., Strauss, J., Günther, F., Grigoriev, M., Maximov, G. M., and Hugelius, G.: Carbon and nitrogen pools in thermokarst-affected permafrost landscapes in Arctic Siberia, Biogeosciences, 15, 953–971, https://doi.org/10.5194/bg-15-953-2018, 2018.

Gérard, F.: Clay minerals, iron/aluminum oxides, and their contribution to phosphate sorption in soils — A myth revisited, Geoderma, 262, 213–226, https://doi.org/10.1016/j.geoderma.2015.08.036, 2016.

Goldman, C. R., Kumagai, M., Robarts, R. D., and Goldman, C. R. (Eds.): Climatic Change and Global Warming of Inland Waters: Impacts and Mitigation for Ecosystems and Societies, John Wiley & Sons Inc, Chichester, West Sussex, UK, 2013.

Harrison, J. C., St-Onge, M. R., Petrov, O. V., Strelnikov, S. I., Lopatin, B. G., Wilson, F. H., Tella, S., Paul, D., Lynds, T., Shokalsky, S. P., Hults, C. K., Bergman, S., Jepsen, H. F., and Solli, A.: Geological map of the Arctic, 2011.

Herndon, E., AlBashaireh, A., Singer, D., Roy Chowdhury, T., Gu, B., and Graham, D.: Influence of iron redox cycling on organo-mineral associations in Arctic tundra soil, Geochimica et Cosmochimica Acta, 207, 210–231, https://doi.org/10.1016/j.gca.2017.02.034, 2017.

Hömberg, A., Obst, M., Knorr, K.-H., Kalbitz, K., and Schaller, J.: Increased silicon concentration in fen peat leads to a release of iron and phosphate and changes in the composition of dissolved organic matter, Geoderma, 374, 114422, https://doi.org/10.1016/j.geoderma.2020.114422, 2020.

Hugelius, G., Strauss, J., Zubrzycki, S., Harden, J. W., Schuur, E. A. G., Ping, C.-L., Schirrmeister, L., Grosse, G., Michaelson, G. J., Koven, C. D., O'Donnell, J. A., Elberling, B., Mishra, U., Camill, P., Yu, Z., Palmtag, J., and Kuhry, P.: Estimated stocks of circumpolar permafrost carbon with quantified uncertainty ranges and identified data gaps, Biogeosciences, 11, 6573–6593, https://doi.org/10.5194/bg-11-6573-2014, 2014.

Hugelius, G., Loisel, J., Chadburn, S., Jackson, R. B., Jones, M., MacDonald, G., Marushchak, M., Olefeldt, D., Packalen, M., Siewert, M. B., Treat, C., Turetsky, M., Voigt, C., and Yu, Z.: Large stocks of peatland carbon and nitrogen are vulnerable to permafrost thaw, Proceedings of the National Academy of Sciences of the United States of America, 117, 20438–20446, https://doi.org/10.1073/pnas.1916387117, 2020.

Jobbágy, E. and Jackson, R. B.: The distribution of soil nutrients with depth: Global patterns and the imprint of plants, Biogeochemistry, 51–77, available at: https://link.springer.com/article/10.1023/A:1010760720215, 2001.

Kaiser, K. and Zech, W.: Competitive Sorption of Dissolved Organic Matter Fractions to Soils and Related Mineral Phases, Soil Sci. Soc. Am. J., 61, 64–69, https://doi.org/10.2136/sssaj1997.03615995006100010011x, 1997.

Köhler, P., Hartmann, J., and Wolf-Gladrow, D. A.: Geoengineering potential of artificially enhanced silicate weathering of olivine, Proceedings of the National Academy of Sciences of the United States of America, 107, 20228–20233, https://doi.org/10.1073/pnas.1000545107, 2010.

Kokelj, S. V. and Burn, C. R.: Geochemistry of the active layer and near-surface permafrost, Mackenzie delta region, Northwest Territories, Canada, Can. J. Earth Sci., 42, 37–48, https://doi.org/10.1139/e04-089, 2005.

Kokelj, S. V., Lantz, T. C., Tunnicliffe, J., Segal, R., and Lacelle, D.: Climate-driven thaw of permafrost preserved glacial landscapes, northwestern Canada, Geology, 45, 371–374, https://doi.org/10.1130/G38626.1, 2017.

Krause, J. W., Duarte, C. M., Marquez, I. A., Assmy, P., Fernández-Méndez, M., Wiedmann, I., Wassmann, P., Kristiansen, S., and Agustí, S.: Biogenic silica production and diatom dynamics in the Svalbard region during spring, Biogeosciences, 15, 6503–6517, https://doi.org/10.5194/bg-15-6503-2018, 2018.

Kuhry, P., Bárta, J., Blok, D., Elberling, B., Faucherre, S., Hugelius, G., Jørgensen, C. J., Richter, A., Šantrůčková, H., and Weiss, N.: Lability classification of soil organic matter in the northern permafrost region, Biogeosciences, 17, 361–379, https://doi.org/10.5194/bg-17-361-2020, available at: https://bg.copernicus.org/articles/17/361/2020/, 2020.

Mann, P. J., Strauss, J., Palmtag, J., Dowdy, K., Ogneva, O., Fuchs, M., Bedington, M., Torres, R., Polimene, L., Overduin, P., Mollenhauer, G., Grosse, G., Rachold, V., Sobczak, W. V., Spencer, R. G. M., and Juhls, B.: Degrading permafrost river catchments and their impact on Arctic Ocean nearshore processes, AMBIO, https://doi.org/10.1007/s13280-021-01666-z, 2022.

Mauclet, E., Agnan, Y., Hirst, C., Monhonval, A., Pereira, B., Vandeuren, A., Villani, M., Ledman, J., Taylor, M., Jasinski, B. L., Schuur, E. A. G., and Opfergelt, S.: Changing sub-Arctic tundra vegetation upon permafrost degradation: impact on foliar mineral element cycling, Biogeosciences, 19, 2333–2351, https://doi.org/10.5194/bg-19-2333-2022, 2022.

Mishra, U., Hugelius, G., Shelef, E., Yang, Y., Strauss, J., Lupachev, A., Harden, J. W., Jastrow, J. D., Ping, C.-L., Riley, W. J., Schuur, E. A. G., Matamala, R., Siewert, M., Nave, L. E., Koven, C. D., Fuchs, M., Palmtag, J., Kuhry, P., Treat, C. C., Zubrzycki, S., Hoffman, F. M., Elberling, B., Camill, P., Veremeeva, A., and Orr, A.: Spatial heterogeneity and environmental predictors of permafrost region soil organic carbon stocks, Science Advances, 7, https://doi.org/10.1126/sciadv.aaz5236, 2021.

Monhonval, A., Strauss, J., Thomas, M., Hirst, C., Titeux, H., Louis, J., Gilliot, A., Du Bois d'Aische, E., Pereira, B., Vandeuren, A., Grosse, G., Schirrmeister, L., Jongejans, L. L.,

Ulrich, M., and Opfergelt, S.: Thermokarst processes increase the supply of stabilizing surfaces and elements (Fe, Mn, Al, and Ca) for mineral–organic carbon interactions, Permafrost Periglac. Process., 33, 452–469, https://doi.org/10.1002/ppp.2162, 2022.

Monhonval, A., Mauclet, E., Pereira, B., Vandeuren, A., Strauss, J., Grosse, G., Schirrmeister, L., Fuchs, M., Kuhry, P., and Opfergelt, S.: Mineral Element Stocks in the Yedoma Domain: A Novel Method Applied to Ice-Rich Permafrost Regions, Front. Earth Sci., 9, https://doi.org/10.3389/feart.2021.703304, 2021.

Mueller, C. W., Rethemeyer, J., Kao-Kniffin, J., Löppmann, S., Hinkel, K. M., and G Bockheim, J.: Large amounts of labile organic carbon in permafrost soils of northern Alaska, Global change biology, 21, 2804–2817, https://doi.org/10.1111/gcb.12876, 2015.

Otsuki, A. and Wetzel, R.: Corprecipitation of phosphate with carbonates in a marl lake, Limnol. Oceanogr., 17, 763–767, https://doi.org/10.4319/lo.1972.17.5.0763, 1972.

Quideau, S. A., Chadwick, O. A., Trumbore, S. E., Johnson-Maynard, J. L., Graham, R. C., and Anderson, M. A.: Vegetation control on soil organic matter dynamics, Organic Geochemistry, 32, 247–252, https://doi.org/10.1016/S0146-6380(00)00171-6, 2001.

R Core Team: R: A language and environment for statistical, R Foundation for Statistical Computing, Vienna, Austria, 2022.

Reimann, C. and Melezhik, V.: Metallogenic provinces, geochemical provinces and regional geology Ð what causes large-scale patterns in low density geochemical maps of the C-horizon of podzols in Arctic Europe?, Applied Geochemistry, 963–983, 2001.

Reithmaier, G.-M. S., Knorr, K.-H., Arnhold, S., Planer-Friedrich, B., and Schaller, J.: Enhanced silicon availability leads to increased methane production, nutrient and toxicant mobility in peatlands, Scientific reports, 7, 8728, https://doi.org/10.1038/s41598-017-09130-3, 2017.

Rengel, Z.: Aluminium cycling in the soil-plant-animal-human continuum, Biometals, 17, 669–689, https://doi.org/10.1007/s10534-004-1201-4, available at: https://idp.springer.com/authorize/casa?redirect_uri=https://link.springer.com/article/10.1007/s10534-004-1201-4&casa_token=iynido51bjuaaaaa:yfvkipyiiyks3if7mhcg2ugd63try1uopdccapkpfve5kfveqapnrobex9t_loo197dhtolwi5kclepeqq, 2004.

Romanovsky, V. E., Drozdov, D. S., Oberman, N. G., Malkova, G. V., Kholodov, A. L., Marchenko, S. S., Moskalenko, N. G., Sergeev, D. O., Ukraintseva, N. G., Abramov, A. A., Gilichinsky, D. A., and Vasiliev, A. A.: Thermal state of permafrost in Russia, Permafrost Periglac. Process., 21, 136–155, https://doi.org/10.1002/ppp.683, 2010.

Salmon, V. G., Soucy, P., Mauritz, M., Celis, G., Natali, S. M., Mack, M. C., and Schuur, E. A. G.: Nitrogen availability increases in a tundra ecosystem during five years of experimental permafrost thaw, Global change biology, 22, 1927–1941, https://doi.org/10.1111/gcb.13204, 2016.

Sanders, T., Fiencke, C., Fuchs, M., Haugk, C., Juhls, B., Mollenhauer, G., Ogneva, O., Overduin, P., Palmtag, J., Povazhniy, V., Strauss, J., Tuerena, R., Zell, N., and Dähnke, K.: Seasonal nitrogen fluxes of the Lena River Delta, Ambio, 51, 423–438, https://doi.org/10.1007/s13280-021-01665-0, available at: https://link.springer.com/article/10.1007/s13280-021-01665-0, 2022.

Schaller, J. and Goeckede, M.: Pan-Arctic soil element availability estimations, available at: doi: 637 https://doi.org/10.17617/3.8KGQUN, 2022.

Schaller, J., Puppe, D., Kaczorek, D., Ellerbrock, R., and Sommer, M.: Silicon Cycling in Soils Revisited, MDPI Plants, 10, https://doi.org/10.3390/plants10020295, 2021a.

Schaller, J., Puppe, D., Kaczorek, D., Ellerbrock, R., and Sommer, M.: Silicon Cycling in Soils Revisited, Plants, 10, 295, https://doi.org/10.3390/plants10020295, available at: https://www.mdpi.com/986170, 2021b.

Schaller, J., Faucherre, S., Joss, H., Obst, M., Goeckede, M., Planer-Friedrich, B., Peiffer, S., Gilfedder, B., and Elberling, B.: Silicon increases the phosphorus availability of Arctic soils, Scientific reports, 9, 449, https://doi.org/10.1038/s41598-018-37104-6, 2019.

Schirrmeister, L., Kunitsky, V., Grosse, G., Wetterich, S., Meyer, H., Schwamborn, G., Babiy, O., Derevyagin, A., and Siegert, C.: Sedimentary characteristics and origin of the Late Pleistocene Ice Complex on north-east Siberian Arctic coastal lowlands and islands – A review, Quaternary International, 241, 3–25, https://doi.org/10.1016/j.quaint.2010.04.004, 2011.

Schneider, M., Scheel, T., Mikutta, R., van Hees, P., Kaiser, K., and Kalbitz, K.: Sorptive stabilization of organic matter by amorphous Al hydroxide, Geochimica et Cosmochimica Acta, 74, 1606–1619, https://doi.org/10.1016/j.gca.2009.12.017, 2010.

Schuur, E. A. G., McGuire, A. D., Schädel, C., Grosse, G., Harden, J. W., Hayes, D. J., Hugelius, G., Koven, C. D., Kuhry, P., Lawrence, D. M., Natali, S. M., Olefeldt, D., Romanovsky, V. E., Schaefer, K., Turetsky, M. R., Treat, C. C., and Vonk, J. E.: Climate change and the permafrost carbon feedback, Nature, 520, 171–179, https://doi.org/10.1038/nature14338, available at: https://www.nature.com/articles/nature14338, 2015.

Schuur, E. A. G., Abbott, B. W., Bowden, W. B., Brovkin, V., Camill, P., Canadell, J. G., Chanton, J. P., Chapin, F. S., Christensen, T. R., Ciais, P., Crosby, B. T., Czimczik, C. I., Grosse, G., Harden, J., Hayes, D. J., Hugelius, G., Jastrow, J. D., Jones, J. B., Kleinen, T., Koven, C. D., Krinner, G., Kuhry, P., Lawrence, D. M., McGuire, A. D., Natali, S. M., O'Donnell, J. A., Ping, C. L., Riley, W. J., Rinke, A., Romanovsky, V. E., Sannel, A. B. K., Schädel, C., Schaefer, K., Sky, J., Subin, Z. M., Tarnocai, C., Turetsky, M. R., Waldrop, M. P., Walter Anthony, K. M., Wickland, K. P., Wilson, C. J., and Zimov, S. A.: Expert assessment of vulnerability of permafrost carbon to climate change, Climatic Change, 119, 359–374, https://doi.org/10.1007/s10584-013-0730-7, 2013.

Schweger, C. E.: LATE PLEISTOCENE VEGETATION OF EASTERN BERINGIA: POLLEN ANALYSIS OF DATED ALLUVIUM, in: Paleoecology of Beringia, Elsevier, 95–112, https://doi.org/10.1016/B978-0-12-355860-2.50013-2, 1982.

Sher, A. V., Kuzmina, S. A., Kuznetsova, T. V., and Sulerzhitsky, L. D.: New insights into the Weichselian environment and climate of the East Siberian Arctic, derived from fossil insects, plants, and mammals, Quaternary Science Reviews, 24, 533–569, https://doi.org/10.1016/j.quascirev.2004.09.007, 2005.

Sims, J. T.: Comparison of mehlich 1 and mehlich 3 extractants for P, K, Ca, Mg, Mn, Cu and Zn in atlantic coastal plain soils, Communications in Soil Science and Plant Analysis, 20, 1707–1726, https://doi.org/10.1080/00103628909368178, 1989.

Sowers, T. D., Wani, R. P., Coward, E. K., Fischel, M. H. H., Betts, A. R., Douglas, T. A., Duckworth, O. W., and Sparks, D. L.: Spatially Resolved Organomineral Interactions across a Permafrost Chronosequence, Environmental science & technology, 54, 2951–2960, https://doi.org/10.1021/acs.est.9b06558, 2020.

Stimmler, P., Priemé, A., Elberling, B., Goeckede, M., and Schaller, J.: Arctic soil respiration and microbial community structure driven by silicon and calcium, In preparation, 2021.

Strauss, J. (Ed.): Permafrost: Recarbonizing global soils – A technical manual of recommended management practices, Food and Agriculture Organization of the United Nations, Rome, 2021.

Strauss, J., Laboor, S., Schirrmeister, L., Fedorov, A. N., Fortier, D., Froese, D., Fuchs, M., Günther, F., Grigoriev, M., Harden, J., Hugelius, G., Jongejans, L. L., Kanevskiy, M., Kholodov, A., Kunitsky, V., Kraev, G., Lozhkin, A., Rivkina, E., Shur, Y., Siegert, C., Spektor, V., Streletskaya, I., Ulrich, M., Vartanyan, S., Veremeeva, A., Anthony, K. W., Wetterich, S., Zimov, N., and Grosse, G.: Circum-Arctic Map of the Yedoma Permafrost Domain, Front. Earth Sci., 9, https://doi.org/10.3389/feart.2021.758360, 2021.

Strauss, J., Schirrmeister, L., Grosse, G., Fortier, D., Hugelius, G., Knoblauch, C., Romanovsky, V., Schädel, C., Schneider von Deimling, T., Schuur, E. A., Shmelev, D., Ulrich, M., and Veremeeva, A.: Deep Yedoma permafrost: A synthesis of depositional characteristics and carbon vulnerability, Earth-Science Reviews, 172, 75–86, https://doi.org/10.1016/j.earscirev.2017.07.007, 2017a.

Strauss, J., Schirrmeister, L., Grosse, G., Fortier, D., Hugelius, G., Knoblauch, C., Romanovsky, V., Schädel, C., Schneider von Deimling, T., Schuur, E. A., Shmelev, D., Ulrich, M., and Veremeeva, A.: Deep Yedoma permafrost: A synthesis of depositional characteristics and carbon vulnerability, Earth-Science Reviews, 172, 75–86, https://doi.org/10.1016/j.earscirev.2017.07.007, 2017b.

Strauss, J., Schirrmeister, L., Grosse, G., Wetterich, S., Ulrich, M., Herzschuh, U., and Hubberten, H.-W.: The deep permafrost carbon pool of the Yedoma region in Siberia and Alaska, Geophysical research letters, 40, 6165–6170, https://doi.org/10.1002/2013GL058088, 2013.

Street, L. E., Mielke, N., and Woodin, S. J.: Phosphorus Availability Determines the Response of Tundra Ecosystem Carbon Stocks to Nitrogen Enrichment, Ecosystems, 21, 1155–1167, https://doi.org/10.1007/s10021-017-0209-x, 2018.

Terhaar, J., Lauerwald, R., Regnier, P., Gruber, N., and Bopp, L.: Around one third of current Arctic Ocean primary production sustained by rivers and coastal erosion, Nature communications, 12, 169, https://doi.org/10.1038/s41467-020-20470-z, 2021.

Tremblay, J.-É., Anderson, L. G., Matrai, P., Coupel, P., Bélanger, S., Michel, C., and Reigstad, M.: Global and regional drivers of nutrient supply, primary production and CO2 drawdown in the changing Arctic Ocean, Progress in Oceanography, 139, 171–196, https://doi.org/10.1016/j.pocean.2015.08.009, 2015.

Villani, M., Mauclet, E., Agnan, Y., Druel, A., Jasinski, B., Taylor, M., Schuur, E. A., and Opfergelt, S.: Mineral element recycling in topsoil following permafrost degradation and a vegetation shift in sub-Arctic tundra, Geoderma, 421, 115915, https://doi.org/10.1016/j.geoderma.2022.115915, 2022.

Walker, D., Bockheim, J., Chapin III, F., Eugster, W., Nelson, F., and Ping, C.: Calcium-rich tundra, wildlife, and the "Mammoth Steppe", Quaternary Science Reviews, 20, 149–163, https://doi.org/10.1016/S0277-3791(00)00126-8, 2001.

Weil, R. R. and Brady, N. C.: The nature and properties of soils, Fifteenth edition, global edition, Pearson, Harlow, England, London, New York, Boston, San Francisco, 1104 pp., 2017.

Wiseman, C. and Püttmann, W.: Interactions between mineral phases in the preservation of soil organic matter, Geoderma, 134, 109–118, https://doi.org/10.1016/j.geoderma.2005.09.001, 2006.

Yang, D. and Kane, D. L. (Eds.): Arctic Hydrology, Permafrost and Ecosystems, Springer eBook Collection, Springer International Publishing; Imprint Springer, Cham, 914 pp., 2021.
Yurchenko, A. Y., Potapova, A. S., Bumagina, V. A., Vilesov, A. P., Chertina, K. N., Balushkina, N. S., Kalmykov, G. A., and Khotylev, O. V.: Morphological and Lithogenetic Classification of the Carbonate Rocks of the Abalak–Bazhenov Complex, Moscow Univ. Geol. Bull., 74, 372–379, https://doi.org/10.3103/S0145875219040136, 2019.
Zabel, M. and Schulz, H. D. (Eds.): Marine Geochemistry, 2nd revised, updated and extended edition, SpringerLink Bücher, Springer Berlin Heidelberg, Berlin, Heidelberg, 574 pp., 2006.